https://doi.org/10.5194/essd-2021-131
Preprint. Discussion started: 26 April 2021

Open Access Earth System Science Data Discussions

Greenland ice sheet mass balance from 1840 through next week

Kenneth D. Mankoff[1], Xavier Fettweis[2], Peter L. Langen[3], Martin Stendel[4], Kristian K. Kjeldsen[1], Nanna B. Karlsson[1], Brice Noël[5], Michiel R. van den Broeke[5], William Colgan[1], Sebastian B. Simonsen[6], Jason E. Box[1], Anne Solgaard[1], Andreas P. Ahlstrøm[1], Signe Bech Andersen[1], and Robert S. Fausto[1]

[1]Department of Glaciology and Climate, Geological Survey of Denmark and Greenland (GEUS), Copenhagen, Denmark
[2]SPHERES research unit, Department of Geography, University of Liège, Liège, Belgium
[3]Department of Environmental Science, iClimate, Aarhus University, Roskilde, Denmark
[4]Department of Climate and Arctic, Danish Meteorological Institute (DMI), Copenhagen, Denmark
[5]Institute for Marine and Atmospheric Research, Utrecht University, The Netherlands
[6]Geodesy and Earth Observation, DTU Space, Technical University of Denmark, Lyngby, Denmark

Correspondence: Ken Mankoff (kdm@geus.dk)

Abstract. The mass of the Greenland ice sheet is declining as mass gain from snowfall is exceeded by mass loss from surface meltwater runoff, marine-terminating glacier calving and submarine melting, and basal melting. Here we use the input/output (IO) method to estimate mass change from 1840 through next week. Mass gains come from three regional climate models (RCMs; HIRHAM/HARMONIE, MAR, and RACMO) and a semi-empirical surface mass balance (SMB) model. Mass losses come from the RCMs, a statistical SMB model, ice discharge at marine terminating glaciers, and ice melted at the base of the ice sheet. From these products we provide an annual estimate of GIS mass balance from 1840 through 1985 and a daily estimate at sector and region scale from 1986 through next week. Compared with other mass balance estimates, this product updates daily, has higher temporal resolution, and is the first IO product to include the basal mass balance which is a source of an additional ~8 % mass loss. Our results demonstrate an accelerating GIS-scale mass loss and general agreement among six other products. Results from this study are available at https://dataverse01.geus.dk/privateurl.xhtml?token=d09976c4-4f89-43ef-8f91-173d269806a4 (Mankoff et al., 2021).

1 Introduction

Over the past several decades, mass loss from the Greenland ice sheet has increased. However, exactly where, when, and how that mass has been lost is not precisely known. There are three common methods for estimating mass balance – changes in gravity (Barletta et al., 2013; Groh et al., 2019; The IMBIE Team, 2019; Velicogna et al., 2020), changes in volume (Simonsen et al., 2021a; Sørensen et al., 2011; Zwally and Giovinetto, 2011; Sasgen et al., 2012; Smith et al., 2020), or the input/output (IO) method (Colgan et al., 2019; Mouginot et al., 2019; Rignot et al., 2019). Each provides some estimate of where, when, and how the mass is lost or gained, and each method has some limitations. The gravity mass balance (GMB) estimate has very low spatial resolution (where), monthly temporal resolution (when), and no information on the process contributing to changes

https://doi.org/10.5194/essd-2021-131
Preprint. Discussion started: 26 April 2021


Open Access Earth System Science Data Discussions

in mass balance components (how). The volume change (VC) mass balance estimate has higher spatial resolution than GMB (where), lower temporal resolution than GMB (when), and again no information on the process (how).

The IO method has a complex definition of spatial resolution (where). The inputs come from regional climate models (RCMs) and therefore have km-scale spatial resolution much higher than GMB and on the order of VC. However, that spatial resolution is generally reduced in the final output to sector or region scale – still higher than GMB but now lower resolution than VC. The IO temporal resolution (when) is limited by ice velocity data updates, which for the past several years occur more frequently than GMB and VC updates. Finally, the IO method is the only one that can provide insight into the processes (how) by distinguishing between changes in mass gain (e.g., snowfall), and changes in mass loss terms (e.g., surface melting vs. calving). Our IO method is also the first IO product to include the basal mass balance (Karlsson et al., 2021) – a term implicitly included in the GMB and VC methods but neglected by all previous IO estimates.

In this work we introduce the new PROMICE Greenland ice sheet mass balance dataset based on the IO method, updating the previous product from Colgan et al. (2019). IO inputs are the positive SMB fields from one RCM (1840 through 1985) to three RCMs (1986 onward), IO outputs are the negative SMB fields from the same RCM(s), the basal mass balance, and an estimate of dynamic ice discharge. Spatial resolution is effectively per sector (Zwally et al., 2012) or region (Mouginot and Rignot, 2019). Temporal resolution is annual from 1840 through 1985, and daily since 1986. The RCM fields are updated daily and the marine mass balance every 12 days and forecasted. Thus, this study provides an estimate of Greenland mass changes from 1840 through next week.

2 Terminology

We use the following terminology throughout the document:

- 'This Study' refers to the new results presented in this study.
- 'Recent' refers to the new 1986 through next week daily temporal resolution data at region and sector scale
- 'Reconstructed' refers to the adjusted Kjeldsen et al. (2015) annual temporal resolution data at GIS scale data used to extend this product from 1986 back through 1840. The 1986 through 2012 portion of the Kjeldsen et al. (2015) data set is used only to adjust the reconstructed data, then discarded.
- ROI (region of interest) refers to one or more of the ice sheet sectors or regions (Fig. 1).
- Sector refers to one of the Zwally et al. (2012) sectors (Fig. 1), expanded here to cover the RCM ice domains which exist slightly outside these sectors in some locations.
- Region refers to the Mouginot and Rignot (2019) regions (Fig. 1), expanded here to cover the RCM ice domains.
- SMB is the surface mass balance from an RCM.

https://doi.org/10.5194/essd-2021-131
Preprint. Discussion started: 26 April 2021


Open Access Earth System Science Data Discussions

- MMB is the marine mass balance, which in other works is often referred to as solid ice discharge or D. It includes both calving and submarine melting.
- BMB is the basal mass balance. It comes from geothermal flux (BMB_{GF}), frictional heating from ice velocity ($BMB_{friction}$), and viscous heat dissipation (BMB_{VHD}).
- MB is the total mass balance including the BMB term (Eq. 3).
- MB* is the mass balance not including the BMB term (Eq. 4).
- HIRHAM/HARMONIE, MAR, and RACMO refer to the RCMs, which only provide SMB. However, when referencing the different MB products, we use, for example, "MAR MB" rather than repeatedly explicitly stating "MB derived from MAR SMB minus BMB and MMB". The use should be clear from context.

3 Product Description

The output of this work is two NetCDF files and one CSV file containing a time series of mass balance and the components used to calculate mass balance. The only difference between the two NetCDF files is the ROI – one for sectors and one for regions. Each also includes properties summed across the entire ice sheet. This Greenland sum data are also the contents of the CSV file. Each NetCDF file includes the ice sheet mass balance (MB), MB per region of interest (ROI; sector or region), MB per ROI per RCM, ice sheet surface mass balance (SMB), SMB per ROI, ice sheet marine mass balance (MMB), MMB per ROI, ice sheet basal mass balance (BMB), and BMB per ROI.

An example of the output is shown in Fig. 2, where the top panel shows mass balance for the entire Greenland ice sheet, in addition to SMB, and MMB, at annual resolution. The lower panel shows an example two years at daily temporal resolution. Because this is ice-sheet-wide, the product includes the reconstructed data to 1840. At sector or region scale, only recent data are provided (Fig. 1).

4 Data Sources

This section introduces data products that exist prior to and external to this work. In the following Methods section we introduce both the intermediate products we generate using these data sources, and the final product that is the output of This Study.

The inputs to this work are the recent SMB fields from the three RCMs, the recent marine mass balance data from Mankoff et al. (2020b) (data: Mankoff and Solgaard (2020b)), and the recent basal mass balance fields, of which BMB_{GF} and $BMB_{friction}$ are direct outputs from Karlsson et al. (2021) (data: Karlsson (2021)), but the BMB_{VHD} calculations are redone here (see Methods Sect. 5.3) using the MAR runoff field. The reconstructed data (pre 1986) are surface and marine mass balance from Kjeldsen et al. (2015) (data: Box et al. (2021)), but adjusted here using the overlapping period (see Methods Sect. 5.4), and runoff from Kjeldsen et al. (2015) (data: Box et al. (2021)) as a proxy and scaled for BMB_{VHD} (see Methods Sect. 5.3).

https://doi.org/10.5194/essd-2021-131
Preprint. Discussion started: 26 April 2021

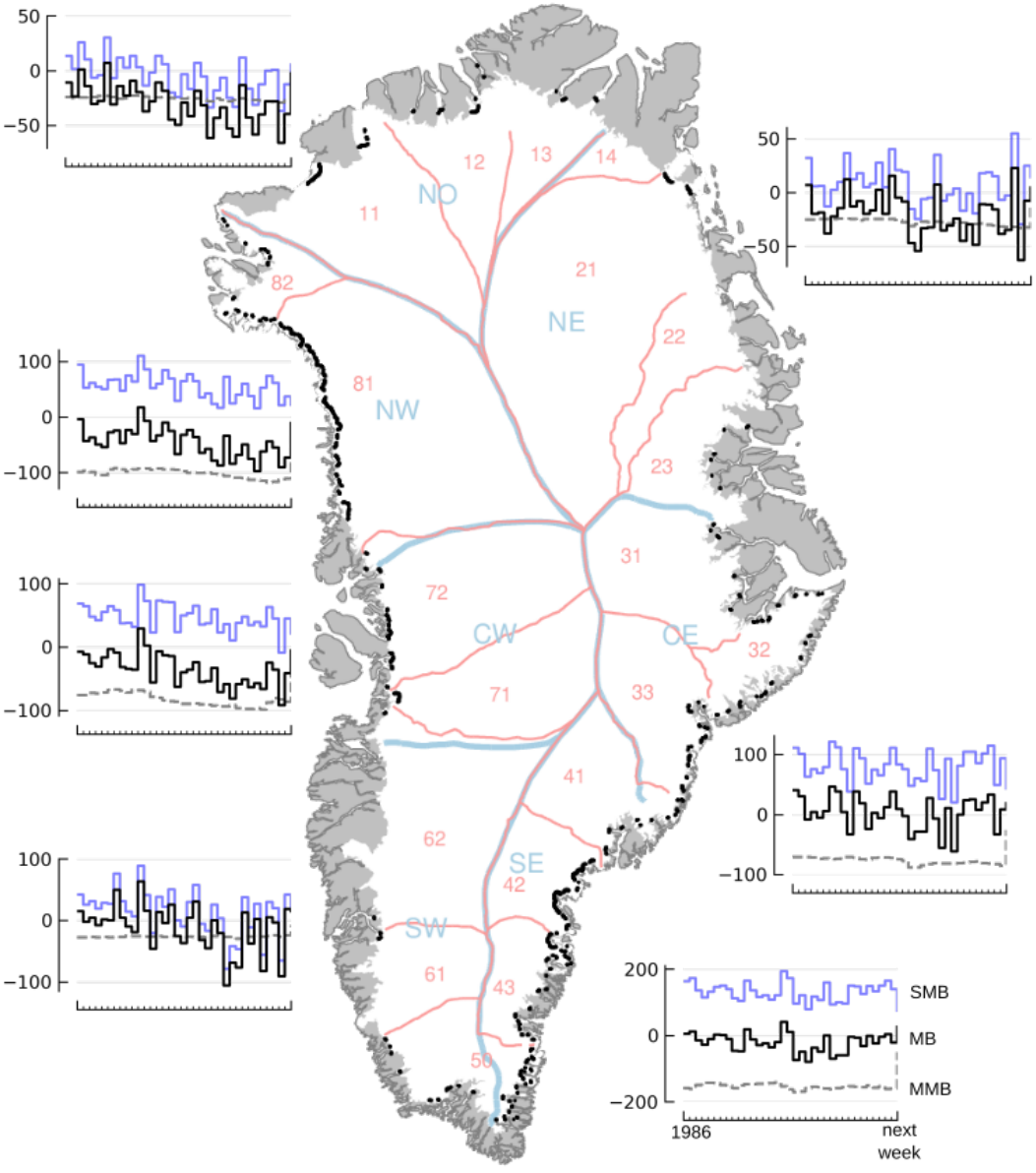

Figure 1. Annual mass balance (black lines), surface mass balance (blue lines) and marine plus basal mass balance (dashed grey) for each of the seven Mouginot and Rignot (2019) regions. The map shows both the named regions (Mouginot and Rignot, 2019) and the numbered sectors (Zwally et al., 2012). Marine mass balance gates are the black blobs near glacier termini. Only recent (post-1986) data are shown because reconstructed data are not separated into regions or sectors. Next week is defined as `2021-05-01` based on the date this document was compiled.

https://doi.org/10.5194/essd-2021-131
Preprint. Discussion started: 26 April 2021

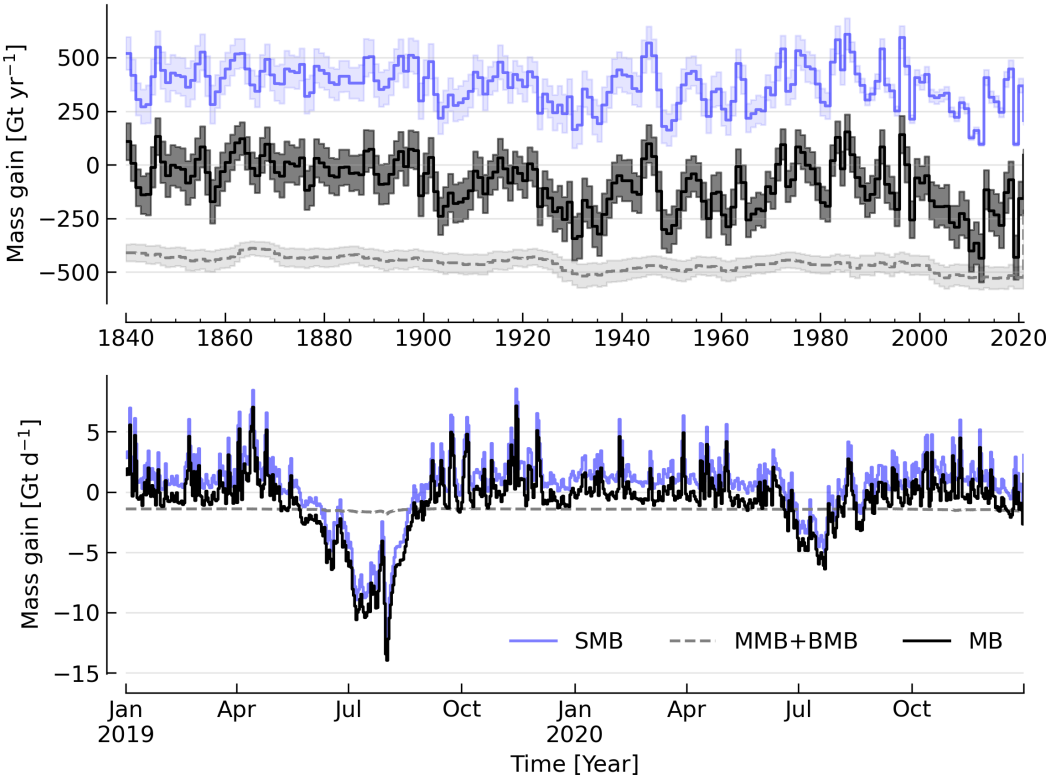

Figure 2. Mass balance and its major components. Top panel: Annual average surface mass balance (blue line), marine mass balance (gray dashed), and their mass balance sum (black line). Here the marine and basal mass balance (MMB + BMB) are shown with sign inverted (e.g. -1 × (MMB+BMB)) Lower panel: Same data at daily resolution and limited to 2019 and 2020.

4.1 Surface mass balance

We use one reconstructed SMB from 1840 through 1985, and three recent SMB from 1986 through last month (HIRHAM/HARMONIE, MAR, and RACMO), two through yesterday (HIRHAM/HARMONIE and MAR) and one through next week (MAR).

4.1.1 HIRHAM/HARMONIE

The HIRHAM/HARMONIE product from the Danmarks Meteorologiske Institut (Danish Meteorological Institute; DMI) is based on an offline subsurface firn/SMB model (Langen et al., 2017), which is forced with surface fluxes of energy (turbulent and downward radiative) and mass (snow, rain, evaporation, and sublimation). These surface fluxes are derived from the HIRHAM5 regional climate model for the reconstructed part of the simulation and from DMI's operational numerical weather forecast model HARMONIE (Iceland-Greenland domain "B", which covers Iceland, Greenland, and the adjacent seas) for the real-time part. HIRHAM5 is used until 2017-08-31 after which HARMONIE is used.

https://doi.org/10.5194/essd-2021-131
Preprint. Discussion started: 26 April 2021


Open Access Earth System Science Data Discussions

The HIRHAM5 regional climate model (Bøssing Christensen et al., 2007) combines the dynamical core of the HIRLAM7 numerical weather forecasting model (Eerola, 2006) with physics schemes from the ECHAM5 general circulation model (Roeckner et al., 2003). In the Greenland setup employed here (Lucas-Picher et al., 2012), it has a horizontal resolution of 0.05 ° x 0.05 ° on a rotated pole grid (corresponding to 5.5 km resolution), and 31 atmospheric levels in the vertical. It is forced at 6 hr intervals on the lateral boundaries with horizontal wind vectors, temperature, and specific humidity from the ERA-Interim reanalysis (Dee et al., 2011). ERA-Interim sea surface temperatures and sea ice concentration are prescribed in ocean grid points. Surface fluxes from HIRHAM5 are passed to the offline subsurface model.

The offline subsurface model was developed to improve firn details for the HIRHAM5 experiments (Langen et al., 2017). The subsurface consists of 32 layers with time-varying fractions of snow, ice and liquid water. Layer thicknesses increase with depth and give a full model depth of 60 m water equivalent. The processes governing the firn evolution include snow densification, varying hydraulic conductivity, irreducible water saturation and other effects on snow liquid water percolation, and retention. Runoff is calculated from liquid water in excess of the irreducible saturation with a characteristic local timescale that depends on surface slope (Zuo and Oerlemans, 1996; Lefebre, 2003). The offline subsurface model is run on the HIRHAM5 5.5 km grid.

For the real-time data we use DMI's operational numerical weather forecast model HARMONIE (Bengtsson et al., 2017), a nonhydrostatic model in terrain-following sigma coordinates based on the fully compressible Euler equations (Simmons and Burridge, 1981; Laprise, 1992). HARMONIE is run at 2.5 km horizontal resolution and with 65 vertical levels. Compared to previous model versions, upper air 3D variational data assimilation of satellite wind and radiance data, radio occultation data, radiosonde, aircraft, and surface observations are incorporated. This is important, as there are only few in situ observations in Greenland. The model is driven at the boundaries with European Centre for Medium-Range Weather Forecasts (ECMWF) high-resolution data at 9 km resolution. The 2.5 km HARMONIE output is regridded to the 5.5 km HIRHAM grid before input to the offline subsurface model.

4.1.2 MAR

The Modèle Atmosphérique Régional (MAR) RCM has been developed by the University of Liège (Belgium) with a focus on the polar regions. The MAR atmosphere model is fully coupled with a snow energy balance model simulating the evolution of the 25 first meters of snow/ice. See Fettweis et al. (2020) for a full description and validation of MAR over Greenland. At its lateral boundary, MAR is 6 hourly forced by the reanalysis NCEP-NCARv1 and run at a resolution of 20 km using the same setup as presented by Tedesco and Fettweis (2020), but using MARv3.11.5 for This Study, while Fettweis et al. (2020) and Tedesco and Fettweis (2020) used MARv3.9 and GridMARv3.10, respectively. The main improvements of MARv3.11 are the inclusion of a blowing snow module (however, not used over Greenland) in addition to small improvements and bug corrections with the aim of improving the evaluation of MAR (with in situ and satellite product) as presented in Fettweis et al. (2020).

In addition to providing SMB, MAR also provides daily runoff – this is used for the daily BMB_{VHD} estimate (Section 5.3).

https://doi.org/10.5194/essd-2021-131
Preprint. Discussion started: 26 April 2021

As the recent SMB decrease (successfully evaluated with GRACE based estimates in Fettweis et al. (2020)) has been fully driven by the increase of runoff, we can assume the same degree of accuracy between SMB simulated by MAR (evaluated with the PROMICE SMB database (Fettweis et al., 2020)) and the runoff simulated by MAR.

Weather-forecasted SMB: To provide a real-time state of the Greenland ice sheet, MAR is forced automatically everyday by the run of 00h UTC from the Global Forecast System (GFS) model providing weather forecasting initialised by the snowpack behaviors of the MAR run from the previous day. This continuous GFS forced time series (without any reinitialisation of MAR) provides SMB estimates between the period covered by NCEP-NCAR and the next 7 days. At the end of each day, NCEP-NCARv1 is used to update the GFS forced MAR time series until about 5 days before the current date and to provide an homogeneous NCEP-NCARv1 forced MAR times series from 1948 to a few days before the current date. We use both the forecasted SMB and runoff fields.

4.1.3 RACMO

The Regional Atmospheric Climate MOdel (RACMO) v2.3p2 has been developed at the Koninklijk Nederlands Meteorologisch Instituut (Royal Netherlands Meteorological Institute; KNMI). It incorporates the dynamical core of the High-Resolution Limited Area Model (HIRLAM) and the physics parameterizations of the ECMWF Integrated Forecast System cycle CY33r1. A polar version (p) of RACMO has been developed at the Institute for Marine and Atmospheric research of Utrecht University (UU-IMAU), to assess the surface mass balance of glaciated surfaces. The current version RACMO2.3p2 has been described in detail in Noël et al. (2018), and here we repeat the main characteristics.

The ice sheet has an extensive dry interior snow zone, a relatively narrow runoff zone along the low-lying margins, and a percolation zone of varying width in between. To capture these processes in first order, the original single-layer snow model in RACMO has been replaced by a 40-layer snow scheme that includes expressions for dry snow densification and a simple tipping bucket scheme to simulate meltwater percolation, retention, refreezing, and runoff (Ettema et al., 2010). The snow layers are initialized in September 1957 using temperature and density from a previous run with the offline IMAU Firn Densification Model (Ligtenberg et al., 2018). To simulate drifting snow transport and sublimation, Lenaerts et al. (2012) implemented a drifting snow scheme. Snow albedo depends on snow grain size, cloud optical thickness, solar zenith angle, and impurity content (van Angelen et al., 2012). Bare ice albedo is assumed constant and estimated as the fifth percentile value of albedo time series (2000-2015) from the 500 m resolution MODIS 16-day albedo product (MCD43A3). Minimum/maximum values of 0.30/0.55 are applied to the bare ice albedo, representing ice with high/low impurity content (cryoconite, algae).

To simulate as accurately as possible the contemporary climate and surface mass balance of the ice sheet, the following boundary conditions have been applied. The glacier ice mask and surface topography have been down-sampled from the 90 m resolution Greenland Ice Mapping Project (GIMP) digital elevation model (DEM; Howat et al. (2014)). At the lateral boundaries, model temperature, specific humidity, pressure, and horizontal wind components at the 40 vertical model levels are relaxed towards 6-hourly ECMWF reanalysis (ERA) data. For this we use ERA-40 between 1958 and 1978 (Uppala et al., 2005), ERA-Interim between 1979 and 1989 (Dee et al., 2011), and ERA-5 between 1990 and 2020 (Hersbach et al., 2020). The relaxation zone is 24 grid cells (~130 km) wide to ensure a smooth transition to the domain interior. This run has active

https://doi.org/10.5194/essd-2021-131
Preprint. Discussion started: 26 April 2021

upper atmosphere relaxation (van de Berg and Medley, 2016). Over glaciated grid points, surface aerodynamic roughness is assumed constant for snow (1 mm) and ice (5 mm). In this run, RACMO2.3p2 has 5.5 km horizontal resolution over Greenland and the adjacent oceans and land masses, but it was found previously that this is insufficient to resolve the many narrow outlet glaciers. The 5.5 km product is therefore statistically downscaled onto a 1 km grid sampled from the GIMP DEM (Noël et al., 2019), employing corrections for biases in elevation and bare ice albedo using a MODIS albedo product at 1 km resolution (Noël et al., 2016).

4.1.4 Reconstructed

The Kjeldsen et al. (2015) 173-year (1840 through 2012) mass balance reconstruction is based on the Box (2013) 171-year (1840 through 2010) statistical reconstruction. Kjeldsen et al. (2015) add a more sophisticated meltwater retention scheme (Pfeffer et al., 1991); weighting of in situ records in their contribution to the estimated value; dispersal of annual accumulation to monthly; and a later end date, i.e., through 2012.

The Box (2013) 171-year (1840-2010) reconstruction is developed from linear regression parameters that describe the least squares regression between a.) spatially discontinuous in situ monthly air temperature records (Cappelen et al., 2011; Cappelen, 2001; Cappelen et al., 2006; Vinther et al., 2006)) or firn/ice cores (Box et al., 2013) and b.) spatially continuous outputs from regional climate model RACMO version 2.1 (Ettema et al., 2010). A 43-year overlap period (1960 through 2012) with the RACMO data are used to determine regression parameters (slope, intercept) on a 5 km grid cell basis. Temperature data define melting degree days, which have a different coefficient for bare ice than snow cover, determined from hydrological-year cumulative SMB. A fundamental assumption is that the calibration factors, regression slope, and offset for the calibration period 1960 through 2012 are stationary over time for which there is some evidence of in Fettweis et al. (2017). Box et al. (2013) describes the methods in more detail.

The reconstructed surface mass balance is adjusted as described in the Methods Sect. 5.4 (Fig. 3).

4.2 Marine mass balance

The recent marine mass balance data are the discharge (D) product from Mankoff et al. (2020b) (data: Mankoff and Solgaard (2020b)). This product covers all fast-flowing (> 100 m yr-1) marine-terminating glaciers. The marine mass balance in Mankoff et al. (2020b) is computed at flux gates ~5 km upstream from glacier termini (Mankoff, 2020), using a wide range of velocity products, and ice thickness from BedMachine v3 (supplemented in the SE Greenland with ice thickness from Millan et al. (2018)). Discharge across flux gates is derived with a 200 m spatial resolution grid, but then summed and provided at glacier resolution (Mankoff and Solgaard, 2020a). Temporal coverage begins in 1986 with a few velocity estimates, and is now updating each time a new velocity product is released, which is every ~12 days with a ~30 day lag (Solgaard et al., 2021) (data: Solgaard and Kusk (2021)).

Some changes have been implemented since the last publication describing the marine mass balance product in detail (i.e., Mankoff et al. (2020b)). These are minor and include updating the surface elevation change product from 2015 through 2019, updating various MEaSUREs velocity products to their latest version, and updating the PROMICE Sentinel ice velocity product

https://doi.org/10.5194/essd-2021-131
Preprint. Discussion started: 26 April 2021


Open Access Earth System Science Data Discussions

from Edition 1 (doi:10.22008/promice/data/sentinel1icevelocity/greenlandicesheet/v1.0.0) to Edition 2 (Solgaard et al. (2021); Solgaard and Kusk (2021)).

The reconstructed marine mass balance data (Kjeldsen et al., 2015) are estimated via a linear fit between unsmoothed annual marine mass balance spanning 2000 to 2012 (Enderlin et al., 2014) and runoff data from Kjeldsen et al. (2015) using a 6-year trailing average. The physical basis for the marine mass balance parameterization using runoff is described in Box and Colgan (2013). The reconstructed marine mass balance is adjusted as described in the Methods Sect. 5.4.

4.3 Basal mass balance

The basal mass balance (BMB; Karlsson et al. (2021)) comes from mass lost at the bed from geothermal flux (BMB_{GF}), frictional heating ($BMB_{friction}$) from the basal shear velocity, and viscous heat dissipation (BMB_{VHD}) from surface runoff routed to the bed (i.e. the volume of the subglacial conduits formed from surface runoff; Mankoff and Tulaczyk (2017)).

These fields (data: Karlsson (2021)) are provided as steady state annual estimates. We use the BMB_{GF} and $BMB_{friction}$ products and apply 1/365th to each day, each year. Because BMB_{VHD} is proportional to runoff, an annual estimate is not appropriate for this work with daily resolution. We therefore re-calculate the BMB_{VHD}-induced basal melt as described in Methods Sect. 5.3.

4.3.1 Geothermal Flux

Due to a lack of direct observations, the geothermal flux is poorly constrained under most of the Greenland ice sheet. Different approaches have been employed to infer the value of the BMB_{GF} often with diverging results (see e.g., Rogozhina et al. (2012); Rezvanbehbahani et al. (2019)). Lacking substantial validation that favours one BMB_{GF} map over the others, Karlsson et al. (2021) instead use the average of three widely used BMB_{GF} estimates: Fox Maule et al. (2009); Shapiro and Ritzwoller (2004), and Martos et al. (2018). The BMB_{GF} melt rate is calculated as

$$\dot{b}_m = E_{GF}\,\rho_i^{-1}\,L^{-1}, \tag{1}$$

where E_{GF} is available energy at the bed, here the geothermal flux in units W m^{-2}, ρ_i is the density of ice (917 kg m^{-3}), and L is the latent heat of fusion (335 kJ kg^{-1}; Cuffey and Paterson (2010)). BMB_{GF} melting is only calculated where the bed is not frozen. We use MacGregor et al. (2016) and scale Eq. 1 by 0, 0.5, or 1 where the bed is frozen, uncertain, or thawed (respectively).

4.3.2 Friction

This heat term stems from the friction produced as ice slides over the bedrock. The term has only been measured in a handful of places (e.g., Ryser et al. (2014); Maier et al. (2019)) and it is unclear how representative those measurements are on ice-sheet scales. Karlsson et al. (2021) therefore estimate the frictional heating using the Full Stokes Elmer/Ice model that resolves all stresses while relating basal sliding and shear stress using a linear friction law (Gillet-Chaulet et al., 2012; Maier et al., 2021).

https://doi.org/10.5194/essd-2021-131
Preprint. Discussion started: 26 April 2021


Open Access Earth System Science Data Discussions

The model is tuned to match a multi-decadal surface velocity map (Joughin et al., 2018) covering 1995-2015 and it returns an estimated basal friction heat that is used to calculate the basal melt due to friction, similar to Eq. 1:

$$\dot{b}_m = E_f \, \rho_i^{-1} \, L^{-1}, \tag{2}$$

where E_f is energy due to friction. We also apply the 0, 0.5, and 1 scale as used for the $\mathrm{BMB_{GF}}$ term (MacGregor et al., 2016) in order to mask out areas that are likely frozen.

4.4 Other

ROI regions come from Mouginot and Rignot (2019) and ROI sectors come from Zwally et al. (2012).

4.5 Products used for validation

We validate This Study against five other data products. These products are the most similar and recent IO product (Mouginot et al., 2019), the previous PROMICE mass balance product (Colgan et al. (2019); data: Colgan (2021)), the two mostly-independent methods of estimating ice sheet mass change: GMB (Barletta et al. (2013); data: Barletta et al. (2020)) and VC (Simonsen et al. (2021a); data: Simonsen et al. (2021b)), and the IMBIE2 data (The IMBIE Team, 2019). In addition to this we evaluate the reconstructed Kjeldsen et al. (2015) (data: Box et al. (2021)) and This Study data during the overlapping period 1986 through 2012. Results of the validation are in Sect. 6.

5 Methods

The total mass balance for all of Greenland and all the different ROIs involves summing each field (SMB, MMB, BMB) by each ROI, then subtracting the MMB and BMB from the SMB fields, or,

$$MB = SMB - MMB - BMB. \tag{3}$$

Products that do not include the BMB term (i.e., Mouginot et al. (2019); Colgan et al. (2019), and Kjeldsen et al. (2015)) have total mass balance defined as

$$MB^* = SMB - MMB \tag{4}$$

And when comparing This Study to those products, we compare like terms, never comparing our MB to a different product MB^*, except Fig. 4 where all data products are graphed together.

Prior to calculating the mass balance, we perform the following steps.

https://doi.org/10.5194/essd-2021-131
Preprint. Discussion started: 26 April 2021


Open Access Earth System Science Data Discussions

5.1 Surface mass balance

In This Study we generate an output based on each of the three RCMs (HIRHAM/HARMONIE, MAR, and RACMO), however, in addition to these we generate a final and 4th SMB field defined as a combination of 1) the adjusted reconstructed SMB from 1840 through 1985 (Sect. 5.4), and 2) the average of HIRHAM/HARMONIE, MAR, and RACMO from 1986 through a few months ago when RACMO drops out, the average of HIRHAM/HARMONIE and MAR from a few months ago through yesterday, and MAR from yesterday through next week. See the Appendix A for differences among This Study MB and MB derived using each of the RCM SMBs. There is no obvious change or step function at the 1985 to 1986 reconstructed-to-recent change, nor as the RACMO and then HIRHAM/HARMONIE RCMs drop out of the time series, a few months ago and yesterday, respectively.

5.2 Forecasted marine mass balance

We estimate future marine mass balance as steady from the most recent estimate (generally between 2 weeks and 1 month old). Ice discharge changes annually by approximately 6 % over the entire ice sheet (King et al., 2018), suggesting a maximum of one-month change of less than 6 %.

5.3 Basal mass balance

Because Karlsson et al. (2021) provide a steady-state annual-average estimate of the BMB fields, we divide the BMB_{GF} and friction velocity ($BMB_{friction}$) fields by 365 to estimate daily average. This is a reasonable treatment of the BMB_{GF} field, which does not have an annual cycle. The $BMB_{friction}$ field does have a small annual cycle that matches the annual velocity cycle. However, when averaged over all of Greenland, this is only a ~6 % variation (King et al., 2018), and Karlsson et al. (2021) found that basal melt rates are 5 % higher for summer maps. Thus, the intra-annual changes are less than the uncertainty. The BMB BMB_{VHD} field varies significantly throughout the year, because it is proportional to runoff. We therefore generate our own BMB_{VHD} for this study.

To estimate recent BMB_{VHD} we use daily MAR runoff (see Mankoff et al. (2020a)) and BedMachine v3 (Morlighem et al., 2017b, a) to derive subglacial routing pathways, similar to Mankoff and Tulaczyk (2017). We assume that all runoff travels to the bed within the grid cell where it is generated, the bed is pressurized by the load of the overhead ice, and the runoff discharges on the day it is generated. We calculate subglacial routing from the gradient of the subglacial pressure head surface, h, defined as

$$h = z_b + k\frac{\rho_i}{\rho_w}(z_s - z_b), \tag{5}$$

with z_b the basal topography, k the flotation fraction (1), ρ_i the density of ice (917 kg m^{-3}), ρ_w the density of water (1000 kg m^{-3}), and z_s the ice surface. Eq. 5 comes from Shreve (1972), where the hydropotential has units of pascals (Pa), but here it is divided by gravitational acceleration g times the density of water ρ_w to convert the units from pascals to meters (Pa to m).

https://doi.org/10.5194/essd-2021-131
Preprint. Discussion started: 26 April 2021


Open Access Earth System Science Data Discussions

We compute h and from that streams and outlets, and both the pressure and elevation difference between the source and outlet. The energy available for basal melting is the elevation difference (gravitational potential energy) and two-thirds of the pressure difference, with the remaining one third consumed to warm the water to match the changing phase transition temperature (Liestøl, 1956; Mankoff and Tulaczyk, 2017). We assume all energy, E_{VHD} (in Joules), is used to melt ice with

$$b_m = E_{\mathrm{VHD}}\, \rho_i^{-1}\, L^{-1}. \tag{6}$$

Because results are presented per ROI and to reduce the computational load of this daily estimate, we only calculate the integrated energy released between the RCM runoff source cell and the outlet cell, and then assign that to the ROI containing the runoff source cell.

To estimate reconstructed basal mass balance, we treat $\mathrm{BMB_{GF}}$ and $\mathrm{BMB_{friction}}$ as steady state as described at the top of this section. For $\mathrm{BMB_{VHD}}$ we use the fact that VHD comes from runoff by definition, and from this, reconstructed $\mathrm{BMB_{VHD}}$ is calculated using scaled runoff as a proxy. VHD theory suggests that a unit volume of runoff that experiences a 1000 m elevation drop will release enough heat to melt an additional 3 % (Liestøl, 1956). To estimate the scale factor we use the 1986 through 2012 overlap between Kjeldsen et al. (2015) runoff and This Study recent $\mathrm{BMB_{VHD}}$ from MAR runoff described above. The correlation between the two has an r^2 value of 0.78, slope of 0.043, and an intercept of -5 Gt $\mathrm{yr^{-1}}$ (Appendix D). From this, we scale the Kjeldsen et al. (2015) reconstructed runoff by 4.3 % to estimate reconstructed $\mathrm{BMB_{VHD}}$.

5.4 Reconstructed adjustment

We use the reconstructed and recent surface (SMB) and marine (MMB) mass balance overlap from 1986 through 2012 to adjust the reconstructed data. This Study vs reconstructed SMB has a slope of 0.6 and an intercept of 165 Gt $\mathrm{yr^{-1}}$ (Fig. 3 SMB), and This Study vs reconstructed MMB has a slope of 1.1 and an intercept of -6 Gt $\mathrm{yr^{-1}}$ (Fig. 3 MMB). The unadjusted reconstructed data slightly underestimates years with high SMB and overestimates years with low SMB (see 1986, 2010, 2011, and 2012 in Fig. 3 SMB). The unadjusted reconstructed data slightly overestimates years with low MMB and overestimates years with high MMB.

We adjust the reconstructed data until the slope is 1 and the intercept is 0 Gt $\mathrm{yr^{-1}}$ for each of the surface and marine mass balance comparisons (Fig. 3). We then derive the $\mathrm{BMB_{VHD}}$ term for reconstructed basal mass balance (Sect. 5.3 and Appendix D), bring in the other BMB terms (Sect. 5.3), and use Eq. 3 to find the reconstructed mass balance.

For surface mass balance, the adjustment is effectively a rotation around the mean values, with years with low SMB decreasing and years with high SMB increasing after the adjustment. For marine mass balance, years with low MMB are slightly reduced, and years with high MMB have a higher reduction to better match the overlapping estimates.

The adjustment described above treats all biases in the reconstructed data. The primary assumption of our adjustment is that the bias contributions do not change in proportion to each other over time.

Given high correlations, we find it reasonable to attribute the disagreement to the demonstrated too-high biases in accumulation and ablation estimates in the 1840-2012 statistical reconstruction SMB (Fettweis et al., 2020), an offset resulting from

https://doi.org/10.5194/essd-2021-131
Preprint. Discussion started: 26 April 2021

Open Access Earth System Science Data Discussions

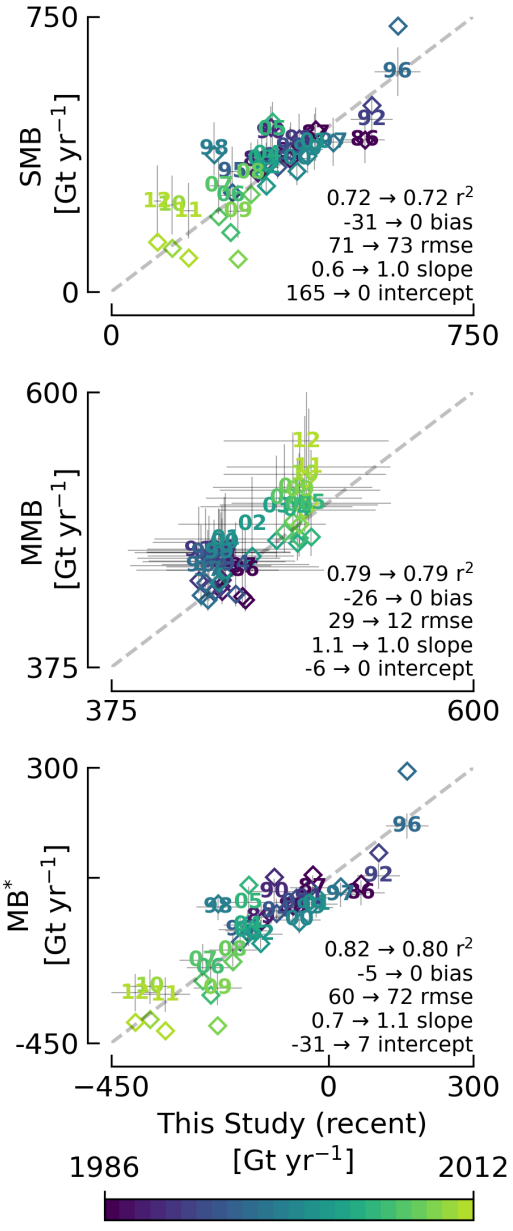

Figure 3. Comparison between This Study and the reconstructed (Kjeldsen et al., 2015) 27-year overlap period. Numbers represent the last two digits of the years for the unadjusted data sets. The matching colored diamonds show the adjusted data. MB* shown here does not include BMB for either the reconstructed or This Study data. Arrows show statistical properties before and after the adjustment. No adjustment is made to MB*, but it is computed from Eq. 4 both before (numbered) and after (diamonds) the surface and marine mass balance adjustments.

https://doi.org/10.5194/essd-2021-131
Preprint. Discussion started: 26 April 2021


Open Access Earth System Science Data Discussions

differences in ice masks (Kjeldsen et al., 2015), other accumulation rate inaccuracies (Lewis et al., 2017, 2019), and other unknowns.

5.5 Domains, Boundaries, and regions of interest

Few of the data products used here are aligned. The Zwally et al. (2012) sectors and the Mouginot and Rignot (2019) regions are often smaller than the RCM ice domains. Cropping the RCM domain edges would remove the edge cells where the largest SMB losses occur. We therefore grow the ROIs to cover the RCM domains. ROIs are grown by expanding them outward, assigning the new cells the value (ROI classification, that is sector number or region name, see Fig. 1) of the nearest non-null cell, and then clipping to the RCM ice domain. This is done for each ROI and RCM.

BMB_{VHD} comes from the MAR ice domain runoff, but is generated on the BedMachine ice thickness grid, which is smaller than the ice domain in some places. Therefore, the largest runoff volumes per unit area (from the low-elevation edge of the ice sheet) are discarded in these locations.

6 Product evaluation and assessment

We compare to six related data sets (see Sect 4.5): The most similar and recent IO product (Mouginot et al., 2019), the previous PROMICE assessment (Colgan et al., 2019), the two mostly independent methods (GMB (Barletta et al., 2013) and VC (Simonsen et al., 2021a)), IMBIE2 (The IMBIE Team, 2019), and the unadjusted reconstructed/recent overlap (Kjeldsen et al., 2015).

Our initial comparison (Fig. 4) shows all seven products overlaid in a time series accumulating at the product resolution (daily to annual) from the beginning of the first overlap (1972, Mouginot et al. (2019)) until seven days from now (now defined as `2021-04-24`). Each data set is manually aligned vertically so that the last timestamps appear to overlap, allowing disagreements to grow back in time. We also assume errors are smallest at present and allow errors to grow back in time. The errors for this product are described in the Uncertainty section.

In the sections below, we compare This Study to each of the validation data in more detail. The Mouginot et al. (2019) and Colgan et al. (2019) products allow term-level (SMB, MMB, and MB^*) comparison, and the GMB, VC, and IMBIE2 only MB-level comparison. The MB or MB^* comparison for each product is summarized in Table 1. All have different masks. Bias [Gt yr^{-1}] is defined as $\frac{1}{n}\sum_{i=1}^{n}(x_i - y_i)$. RMSE [Gt yr^{-1}] is defined as $\sqrt{\frac{1}{n}\sum_{i=1}^{n}(x_i - y_i)^2}$. Sums are computed using ice-sheet wide annual values, where x is This Study, y is the other product, and a positive bias means that This Study has a larger value.

6.1 Mouginot (2019)

The Mouginot et al. (2019) product spans the 1972 through 2018 period. The SMB originates from the RACMO v2.3p2 downscaled at 1 km, and agrees very well with SMB from This Study (r^2 0.97, bias -1, RMSE 18, slope 1.0). The minor SMB differences are likely due to mask differences, our use of a three-RCM average SMB estimate, or perhaps updates to the RACMO model since the Mouginot et al. (2019) study.

https://doi.org/10.5194/essd-2021-131
Preprint. Discussion started: 26 April 2021

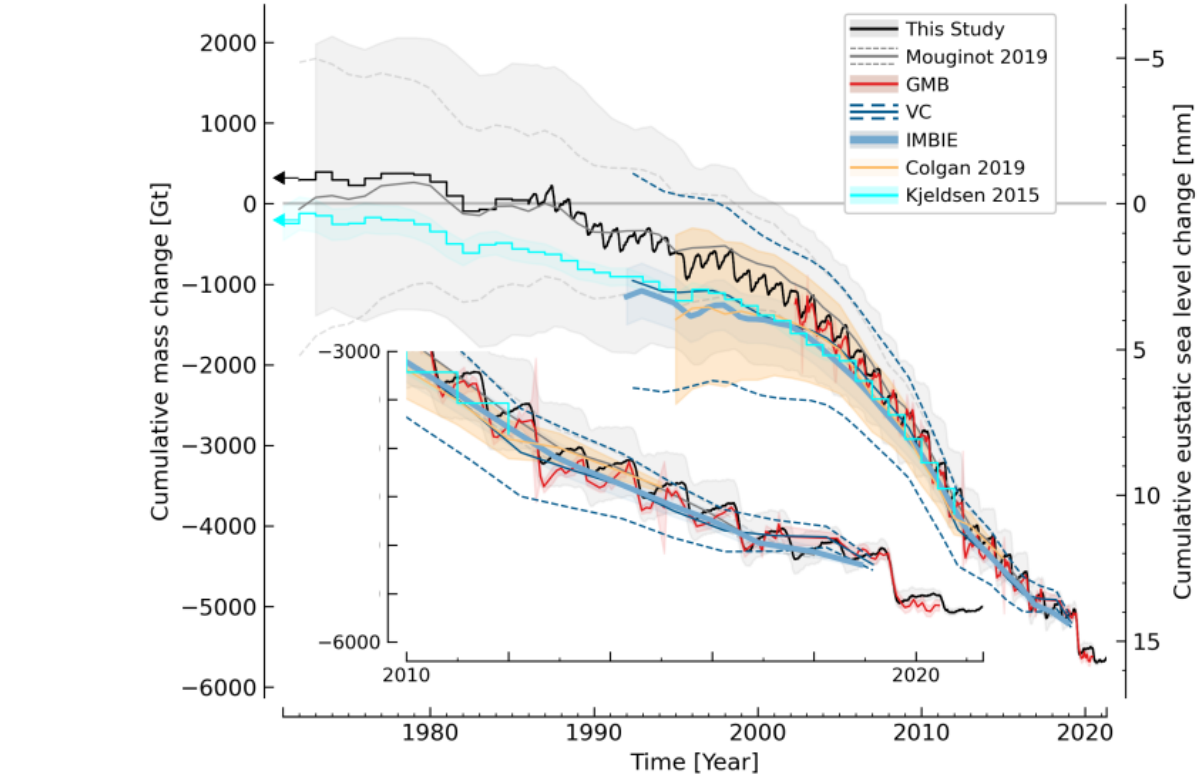

Figure 4. Comparison between This Study and other mass balance time series. Note that various products do or do not include basal mass balance or peripheral glaciers (see Table 1). This Study annual-resolution data prior to 1986 is the Kjeldsen et al. (2015) data adjusted as described in Sect. 5.4. Sea level rise calculated as -Gt/361.8. Inset highlights changes since 2010.

Table 1. Summary of correlation, bias, and RMSE between different products during their overlap periods with This Study.

Other product	r^2	bias	RMSE	Fig.	Notes
Mouginot et al. (2019)	0.96	-4	29	5	No basal mass balance
Colgan et al. (2019)	0.88	-50	69	6	No basal mass balance
GMB	0.87	13	54	7	Includes peripherals
VC	0.64	-29	89	7	Multi-year smooth
IMBIE2	0.89	-25	50	7	No BMB when using IO; BMB when using GMB
Kjeldsen et al. (2015)	0.82	-5	60	3	No basal mass balance; Includes peripherals

335 Mouginot et al. (2019) discharge and our MMB from Mankoff et al. (2020b) have a -23 Gt yr^{-1} bias. This difference can mainly be attributed to different discharge estimates in the Southeast and Central east sector (Appendix: Mouginot regions). When we include BMB in This Study (diamonds in middle panel shifting values to the right), it adds ~25 Gt yr^{-1} to This Study.

https://doi.org/10.5194/essd-2021-131
Preprint. Discussion started: 26 April 2021

Open Access Earth System Science Data Discussions

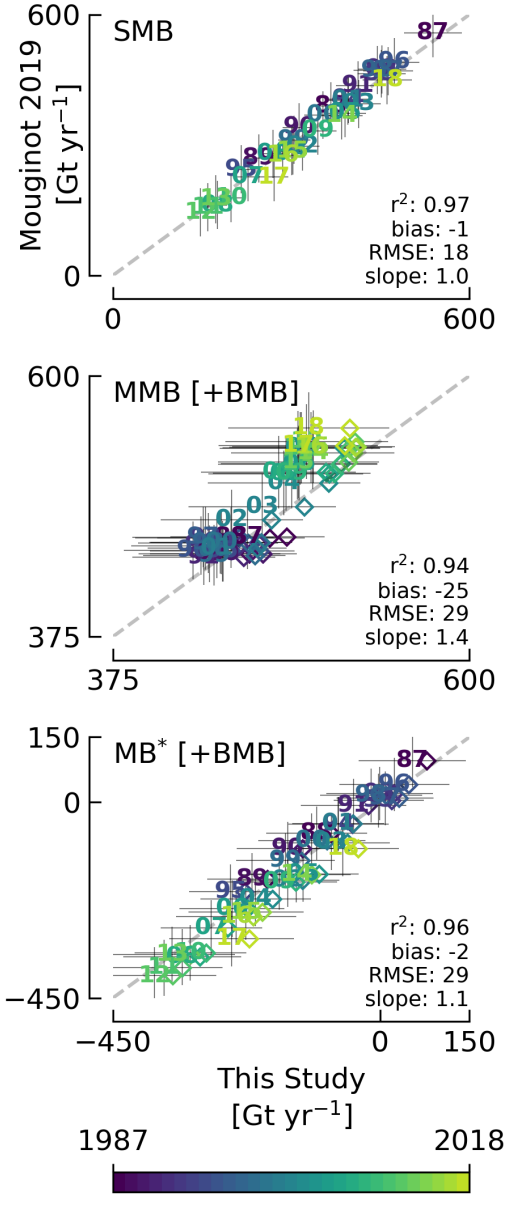

Figure 5. Comparison of This Study vs Mouginot et al. (2019). Numbers represent the last two digits of the year. Matching colored diamonds show the data when BMB is added to This Study. Printed numbers (r^2, bias, RMSE, slope) compare values without BMB.

Because MB* is a linear combination of SMB and MMB terms (Eq 4), the MB* difference between this product and Mouginot et al. (2019) is dominated by the SMB term. The MMB disagreement adds only a small amount of noise to the overall agreement.

https://doi.org/10.5194/essd-2021-131
Preprint. Discussion started: 26 April 2021

Open Access Earth System Science Data Discussions

6.2 Colgan (2019)

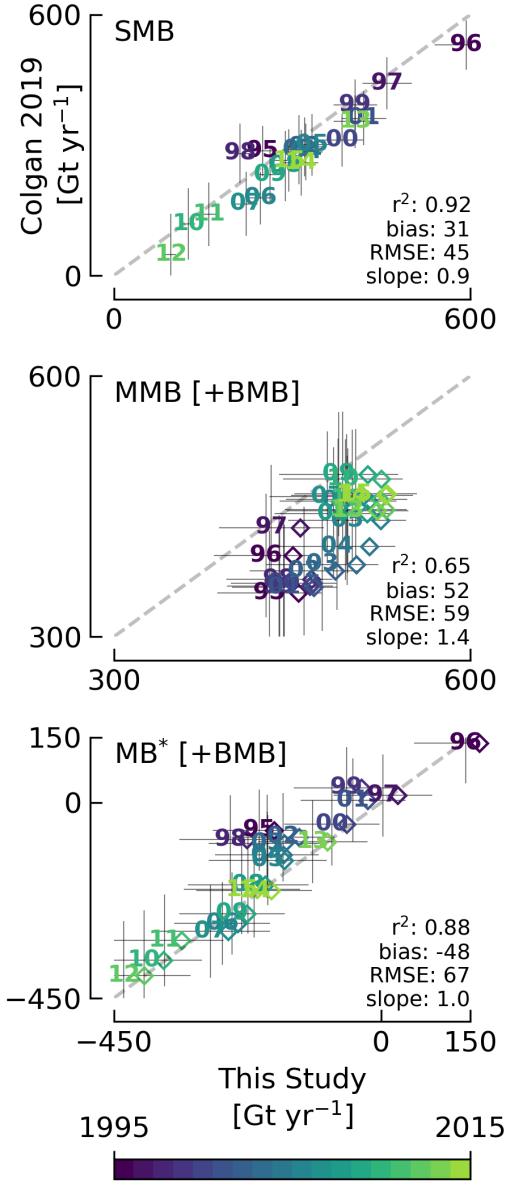

Figure 6. Comparison of This Study vs Colgan et al. (2019). Numbers represent the last two digits of the year. Matching colored diamonds show the data when BMB is added to This Study. Printed numbers (r^2, bias, RMSE, slope) compare values without BMB.

The Colgan et al. (2019) product spans 1995 through 2015. The SMB term is broadly similar to the RCM-averaged SMB term in This Study, although Colgan et al. (2019) use only an older version of MAR (Fig. 6 top panel). The Colgan et al. (2019)

https://doi.org/10.5194/essd-2021-131
Preprint. Discussion started: 26 April 2021

SMB is spatially interpolated over the PROMICE ice-sheet ice mask (Citterio and Ahlstrøm, 2013), which contains more detail on the ice sheet periphery, but also a larger ablation area than the native coarser MAR ice mask. This Study does not interpolate the SMB field and instead works on the SMB ice domain.

The most critical difference between This Study and Colgan et al. (2019) is that the latter estimate grounding line ice discharge based on corrections to ice volume flow rate measured across the approximately 1700 m elevation contour. This ice volume flow rate measurement is far inland relative to the grounding line flux gates used in This Study (from Mankoff (2020)). This introduces large uncertainty in the Colgan et al. (2019) MMB term induced by the SMB corrections between the 1700 m elevation contour and the terminus (see large disagreement in Fig. 6 mid panel). This disagreement increases when BMB is included in the results of This Study (shown by dots shifting the annual values to the right).

The MMB disagreement is represented differently across sectors (Appendix: Colgan 2019), where sectors 1, 2, 5, and 6 all have correlation coefficients less than ~0.1, while the remaining sectors 3, 4, 7, and 8 all have correlation coefficients greater than 0.5.

This Study assesses greater MMB bias (54 Gt yr^{-1}) than Colgan et al. (2019). While Colgan et al. (2019) did not assess BMB, the majority (> 85%) of this discrepancy likely results from Colgan et al. (2019) aliasing the aforementioned downstream correction terms. For example, while This Study shows very little inter-annual variability in ice discharge in the predominantly land-terminating SW region, Colgan et al. (2019) infer large inter-annual variability in ice based on large inter-annual variability in SMB and changes in ablation area ice volume in their Sector 6. The discrepancy between This Study and Colgan et al. (2019) MMB [+BMB] is largest during the earliest part of the record (i.e. 1995-2000), decreasing towards present-day, which may suggest that Colgan et al. (2019) particularly overestimated the response in ice discharge to 1990s climate variability.

Similar to the comparison with Mouginot et al. (2019), the variation in Colgan et al. (2019) MB^* is also ultimately dominated by variation in the SMB term. This leads to strong agreement between this study and the Colgan et al. (2019) estimated annual MB^*.

6.3 Gravimetric Mass Balance (GMB)

The primary difference between GMB and This Study is that the GMB method includes mass losses and gains on peripheral glaciers which should introduce a bias of ~10 to 15 % (Colgan and Arenson, 2013; Bolch et al., 2013), while This Study does not include peripheral glaciers. The inclusion of peripheral glaciers in the GMB product is because the resolution is so low that it cannot distinguish between them and the main ice sheet. There is also signal leakage from other glaciated areas, eg. the Canadian Arctic. This can have a major effect on the estimated signal, especially in sectors 1 and 8 or regions NW and NO. There is also leakage between basins, which becomes a larger issue for smaller basins or where major outlet glaciers are near basin boundaries. GMB may also have an amplified seasonal signal due to changing snow loading in the surrounding land areas that may be mapped as ice sheet mass change variability. This would enhance the seasonal amplitude but not have an impact on the inter-annual mass change rates. Additionally, different glacial isostatic adjustment (GIA) corrections applied to the gravimetric signal may also lead to differences in GMB estimates on ice sheet scale, but also on sector scale (e.g. Sutterley et al. (2014); Khan et al. (2016)).

https://doi.org/10.5194/essd-2021-131
Preprint. Discussion started: 26 April 2021

Open Access Earth System Science Data Discussions

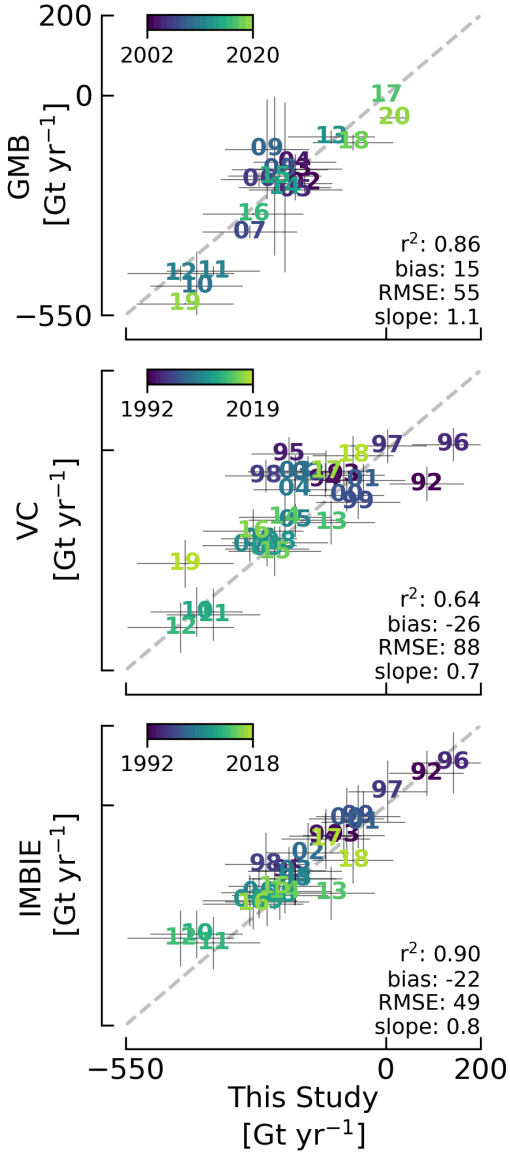

Figure 7. This Study total mass balance (MB) vs. the gravimetric method (GMB), volume change method (VC) and IMBIE2 estimates of MB. All three include BMB. GRACE and IMBIE2 include peripheral glaciers.

GMB and the IO method (This Study) both report changes in ice sheet mass, but they are measuring two fundamentally different things. The IO method tracks volume flow rate across the ice sheet boundary. Typically this is meltwater across the ice sheet surface and solid ice across flux gates near the calving edge of the ice sheet, and in This Study also meltwater across the ice sheet basal boundary. That volume is then converted to mass. We consider that mass 'lost' as soon as it crosses the

https://doi.org/10.5194/essd-2021-131
Preprint. Discussion started: 26 April 2021

boundary (i.e. the ice melts or ice crosses the flux gate). The GMB method tracks the regional mass changes. Melting ice has no impact on this, until the meltwater enters the ocean and a similar mass leaves the far-field GMB footprint. From these differences, the GMB method may be a better estimate of sea level rise, while the I/O method may be a better representation of the state of the Greenland ice sheet.

6.4 Volume change

When deriving surface elevation change from satellite altimetry, data from multiple years are needed to give a stable ice sheet-wide prediction. Hence, the altimetric mass balance estimates are often reported as averages of single satellite missions.

Although This Study has a small (-29 Gt yr^{-1}) bias in comparison to Simonsen et al. (2021a) VC, there is a relatively high RMSE of 89 Gt yr^{-1} and a mid-range correlation (r^2 = 0.64). This suggests that while both This Study and VC agree on the total mass loss of the ice sheet, they disagree on the precise temporal distribution of this mass loss. The 1992 extreme low melt year and the 2019 extreme melt year, as well as the 1996-1998 period, stand out as years of especially poor agreement.

We suggest that this is due to climate influences on the effective radar horizon across the ice sheet during these years. Weather-driven changes in the effective scatter horizon, mapped by Ku-band in the upper snow layer of ice sheets hampers the conversion of radar-derived elevation change into mass change (Nilsson et al., 2015). Simonsen et al. (2021a) used a machine learning approach to derive a temporal calibration field for converting the radar elevation change estimates into mass change. This approach relied on precise mass balance estimates from ICESat to train the model and thereby was able to remove the effects of the changing scattering horizon in the radar data. This VC mass balance is given for monthly time steps (Simonsen et al., 2021a), however the running-mean applied to derive radar elevation change will dampen the interannual variability of the mass balance estimate from VC. This is especially true prior to 2010, after which the novel radar altimeter onboard CryoSat-2 allowed for a shortening of the data windowing from 5 to 3 years. This smoothing of the interannual variability is also seen in the intercomparison between This Study and the VC MB, where in addition to the two end members of the time series (1992 and 2019) the years 1995, 1996, and 1998 seem to be outliers (Fig. 7). These years are notable for high MB which seems to be captured less precisely by the older radar altimeters due to the longer temporal averaging.

6.5 IMBIE

The most widely cited estimate of Greenland mass balance today is the Ice-Sheet Mass Balance Inter-Comparison Exercise 2 (IMBIE2, The IMBIE Team (2019)). IMBIE2 seeks to provide a consensus estimate of monthly Greenland mass balance between 1992 and 2018 that is derived from altimetry, gravimetry, and input-output ensemble members. There are two critical methodological differences between This Study and IMBIE2. Firstly, the gravimetry members of IMBIE2 assesses mass balance of all Greenland land ice, including peripheral ice masses, while This Study only assesses mass balance of the ice sheet proper. Secondly, the input-output members of IMBIE2 do not assess BMB, while This Study does.

Of the 26 independent estimates in the IMBIE2 assessment 9 are from satellite altimetry. Prior to 2003, IMBIE2 is derived using only the IO method (MB is actually MB^*), while after 2003, it is mostly driven by the variability of GRACE dampened by the longer averaging in the altimetry.

https://doi.org/10.5194/essd-2021-131
Preprint. Discussion started: 26 April 2021


Open Access Earth System Science Data Discussions

In comparison to mass balance assessed by IMBIE2, This Study has a small bias of ~ -24 Gt yr^{-1} over the common 26 calendar year comparison period. This apparent agreement may be attributed to the compensating effects of IMBIE2 effectively sampling peripheral ice caps and ignoring BMB, while This Study does the opposite and ignores peripheral ice caps but samples BMB, equal to ~25 Gt yr^{-1}. Over the entire 26-year comparison period, the RMSE with IMBIE2 is ~ 50 Gt yr^{-1} and the correlation is 0.89. This relatively high correlation highlights good agreement in interannual variability between studies, and the RMSE suggests that formal stated uncertainties of each study (c. ±30 to ±63 Gt yr^{-1} for IMBIE2 and mean of 88 Gt yr^{-1} for This Study) are indeed good estimates of the true uncertainty, as assessed by inter-study discrepancies.

7 Uncertainty

We treat the three inputs to the total mass balance (surface, marine, and basal mass balance, or SMB, MMB, and BMB) as independent when calculating the total error. This is a simplification – the RCM SMB and the BMB_{VHD} from RCM runoff are related, and MMB ice thickness and BMB_{VHD} pressure gradients are related, and other terms may have dependencies. However, the two dominant IO terms, SMB inputs and MMB outputs, are independent on annual time scales, and for simplification we treat all terms as independent. We use Eq 3 and standard error propagation for SMB, MMB, and BMB terms (i.e., the square root of the sum of the squares of the SMB plus MMB plus BMB). For the MMB, extra work is done to calculate uncertainty between the last Mankoff 2020 MMB data (up to 30 days old, with error of ~10 % or ~50 Gt yr^{-1}) and the forecasted now-plus-7-day MMB (see Sect. 7.1). Table 2 provides a summary of the uncertainty for each input.

The final This Study MB uncertainty value shown in Table 2 comes from the average value of the MB error term after summing by year and computing the mean of the uncertainty.

7.1 Marine mass balance

The MMB uncertainty is adjusted from the forecasted MMB based on reconstructed the MMB variability. For the forecast period we estimate the uncertainty based on data from all previous years. On the first forecasted day the uncertainty is increased from the baseline approximate 10 % by adding 2 standard deviations of the daily variability in MMB on that calendar date throughout our record. On the second forecasted day we do the same, and then use the larger of that value or the previous days value (i.e., uncertainty cannot decrease as the forecast moves forward in time). We repeat this for the approximately 30 days of forecasted MMB. This implementation takes into account the larger variability (uncertainty) during the seasonal transition between the lower winter and higher summer discharge, or the smaller variability during the winter period.

7.2 Regions of interest (ROI)

Domain and ice mask alignment issues are non-trivial. In general, we work on the three different domains of the three RCMs, and expand the ROIs to match the RCMs. However, some alignment issues cannot be solved. For example, we use BedMachine ice thickness to estimate BMB_{VHD}. Often, the largest BMB_{VHD} occurs near the ice margin under ice with the steepest surface slopes. This is also where the largest runoff often occurs, because the ice margin, at the lowest elevations, is exposed to the

https://doi.org/10.5194/essd-2021-131
Preprint. Discussion started: 26 April 2021

Open Access Earth System Science Data Discussions

Term	Uncertainty [±]	Notes
HIRHAM / HARMONIE SMB	15 %	Langen et al. (2017). The mean accumulation bias (-5%) and ablation bias (-7%) tend to cancel out, but this cannot be expected to be the case on single-basin, short-term scales where uncertainty is estimated to be larger.
MAR SMB	15 %	Fettweis et al. (2020). The mean bias between the model and the measurements was 15 % with a maximum of 1000 mmWE yr^{-1}. GrSMBMIP uses integrated values over several months of SMB, suggesting larger uncertainty of modeled runoff at the daily timescale.
RACMO SMB	15 %	Noël et al. (2019). Average 5% runoff bias compared to annual cumulative discharge from the Watson River. Increases to a maximum of 20 % for extreme runoff years.
This Study SMB	9 %	Average of 15 % SMB uncertainties above, assuming uncorrelated.
Reconstructed SMB	∼ 20 %	From Kjeldsen et al. (2015) Table 1.
Recent MMB	∼ 50 Gt yr^{-1}	∼ 10 %. Mankoff et al. (2020b).
Reconstructed MMB	∼ 10 %	From Kjeldsen et al. (2015) Table 1.
BMB_{GF}	50 %	5.3 +4/-1.4 Gt yr^{-1} from Karlsson et al. (2021) Table 1, using the average of the three available methods.
$BMB_{friction}$	20 %	11.8 ±3.4 Gt yr^{-1} from Karlsson et al. (2021) Table 1.
BMB_{VHD}	15 %	MAR runoff uncertainty.
This Study MB	∼ 88 Gt yr^{-1}	Eq 3, assuming all uncertainty is uncorrelated.

Table 2. Summary of uncertainty estimates for products used in This Study. This is an approximate and simplified representation – RCM uncertainties are calculated separately for gain and loss terms, because SMB near 0 does not mean uncertainty is near 0. This is also why the final This Study uncertainty is presented with units [Gt yr^{-1}].

warmest air. If these RCM ice grid cells with high runoff are anywhere inside the BedMachine ice domain, that runoff is still included in our BMB_{VHD} estimates because it flows outward and passes through the BedMachine near-ice-edge grid cells with the large pressure gradients. However, if these RCM ice grid cells with high runoff are outside the BedMachine ice domain (ice thickness is 0), there is no reasonable way to include that runoff in our BMB_{VHD} budget. It is ignored. We encourage RCM developers, BedMachine, and others to use a common and up-to-date mask (see Kjeldsen et al. (2020)).

7.3 Accumulating uncertainties

When accumulating errors as in Fig. 4, we use only the MMB uncertainty. This is because the MMB uncertainty is primarily due to unknown ice thickness and is invariant in time, and for temporal accumulation, we treat the BMB and SMB uncertainties as random in time.

The shaded region in Fig. 4 representing the uncertainty for This Study is computed as a 365 day rolling smooth from 1840 through 1999, 1/365th of the annual error at now + 7 days, and a linear blend, from 2000 to now + 7 days, between the smoothed reconstructed uncertainty and the present and future more variable uncertainty.

https://doi.org/10.5194/essd-2021-131
Preprint. Discussion started: 26 April 2021


Open Access Earth System Science Data Discussions

The Mouginot et al. (2019), Colgan et al. (2019), and Kjeldsen et al. (2015) all products provide an error estimate, but do not distinguish between temporally fixed errors (biases; should accumulate in time) vs. temporally random errors.

We treat the Mouginot et al. (2019) data the same as This Study. Marine mass balance uncertainty is treated as a bias and accumulates, and surface mass balance uncertainty is treated as random and does not accumulate.

The Colgan et al. (2019) vs. this study bias and RMSE are -50 and 69 Gt yr^{-1} respectively. This suggests that in any given year, there could be up to -50 ± 69 or +19/-119 Gt yr^{-1} departure from This Study. From this, we assign a 50 Gt yr^{-1} bias (42 %; accumulates in time) and a 69 Gt yr^{-1} RMSE (58 %; random in time).

The adjusted Kjeldsen et al. (2015) data have 0 surface and marine mass balance bias by definition (Sect. 5.4), but Fig. 4 displays the unadjusted data, and we use the same method as for the Colgan et al. (2019) data. The unadjusted Kjeldsen et al. (2015) vs. this study bias and RMSE are -5 and 60 Gt yr^{-1} respectively, meaning there could be up to a -5 ± 60 Gt yr^{-1} departure from This Study. We assign a 5 Gt yr^{-1} error to the accumulating data.

7.4 Peripheral Glaciers

Greenland's peripheral glaciers are not included in this product. Nonetheless, we briefly summarize recent mass balance estimates of these areas. Greenland peripheral glaciers contribute more runoff per unit area than the main ice sheet – they are < 5 % of the total ice area but contribute ~15 to 20 % of the whole island mass loss (Bolch et al., 2013). From 2003 to 2009 and using the VC method (altimetry), Gardner et al. (2013) estimate -38 ±7 Gt yr^{-1} peripheral mass balance. From 2006 to 2016 and using the VC method (DEM differencing), Zemp et al. (2020) estimate -51 ±17 Gt yr^{-1} peripheral mass balance, using Rastner et al. (2012) delineations.

When the IO estimate can be applied to these peripheral glaciers (i.e., thickness data becomes available) this product can then include them.

8 Results

From the 181 years of data, the mean mass balance is -90 ±120 Gt yr^{-1}, with a minimum of -434 Gt in 2012 (SMB of 96 ±9 Gt, MMB of 496 ±51 Gt, BMB of 34 ±7 Gt) and a maximum of 152 Gt in 1985 (SMB of 609 ±74 Gt, MMB of 433 ±34 Gt, BMB of 24 ±12 Gt).

At the decadal average, the following trends are apparent. Surface mass balance has decreased from a high of ~450 Gt yr^{-1} in the 1860s to low of ~260 Gt yr^{-1} in the 2010s. SMB variability has also increased during this time. Marine mass balance has increased slightly from a low of ~330 Gt yr^{-1} in the 1860s to a high of ~500 Gt yr^{-1} in the 2010s. Basal mass balance has increased by ~15 % from a low of 24 Gt yr^{-1} in the 1860s to a high of ~28 Gt yr^{-1} in the 2010s.

The total mass balance decadal trend from 1840 through 2020 is one of general mass decrease and increased inter-decadal variability. The record begins in the 1840s with ~-20 Gt yr^{-1}, has only one (of 19) decades with a mass gain of ~40 Gt yr^{-1} in the 1860s, and a record low of ~-270 Gt yr^{-1} in the 2010s.

https://doi.org/10.5194/essd-2021-131
Preprint. Discussion started: 26 April 2021

9 Data availability

The RCM surface mass balance, the marine mass balance, and the VHD basal mass balance components are updated daily, and used to produce the final daily-updating product. The data area available at https://dataverse01.geus.dk/privateurl.xhtml?token=d09976c4-4f89-43ef-8f91-173d269806a4 while the paper is in review, and will be available at https://doi.org/10.22008/FK2/YG3IWC (Mankoff et al., 2021), with all historical versions archived, after review.

As part of our commitment to make continual and improving updates to the data product, we introduce a GitHub database (https://github.com/GEUS-PROMICE/mass_balance/issues/; last visited 2020-04-01) where users can track progress, make suggestions, discuss, and report and respond to issues that arise during use of this product.

10 Conclusions

This study is the first to provide a dataset containing more than century and real time estimates detailing the state of Greenland ice sheet mass balance, with regional or sector spatial and daily temporal resolution products of surface mass balance, marine mass balance, basal mass balance, and the total mass balance.

IMBIE2 highlights that during the GRACE satellite gravimetry era (2003 through 2017), there are usually more than twenty independent estimates of annual Greenland ice sheet mass balance. Just two independent estimates, however, are available prior to 2003. This study will therefore provide additional insight on ice sheet mass balance during the late 1980s and 1990s. IMBIE2 also highlights how the availability of mass balance estimates declines in the year prior to IMBIE2 publication. This reflects a lag period during which mass balance assessments from non-operational products are undergoing peer-review. The operational nature of this product supports the timely inclusion of annual MB estimates in community consensus reports such as those from IMBIE and the IPCC.

As such, the data products provided in this study present the first operational monitoring of the Greenland ice sheet total mass balance and its components. One property of the input-output approach used in This Study is the explanatory capabilities of the data products, allowing scrutiny of the physical origins of recorded mass changes. By excluding peripheral ice masses, this study allows and invites anyone to keep an eye on the current evolution of the Greenland ice sheet proper. However, as the spatial resolution of RCM increases and estimates of ice thickness of the peripheral glacier become available, our setup allows inclusion of these ice masses to generate a full Greenland-wide product. Moreover, as the determination of each of the individual components of the ice sheet mass balance is expected to improve over time through international research efforts, the total mass balance product presented will also be able to improve, as it is sustained by the Danish-Greenlandic governmental long-term monitoring effort – the Programme for Monitoring of the Greenland ice sheet (PROMICE).

https://doi.org/10.5194/essd-2021-131
Preprint. Discussion started: 26 April 2021

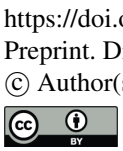

Open Access Earth System Science Data Discussions

Appendix A: RCM differences

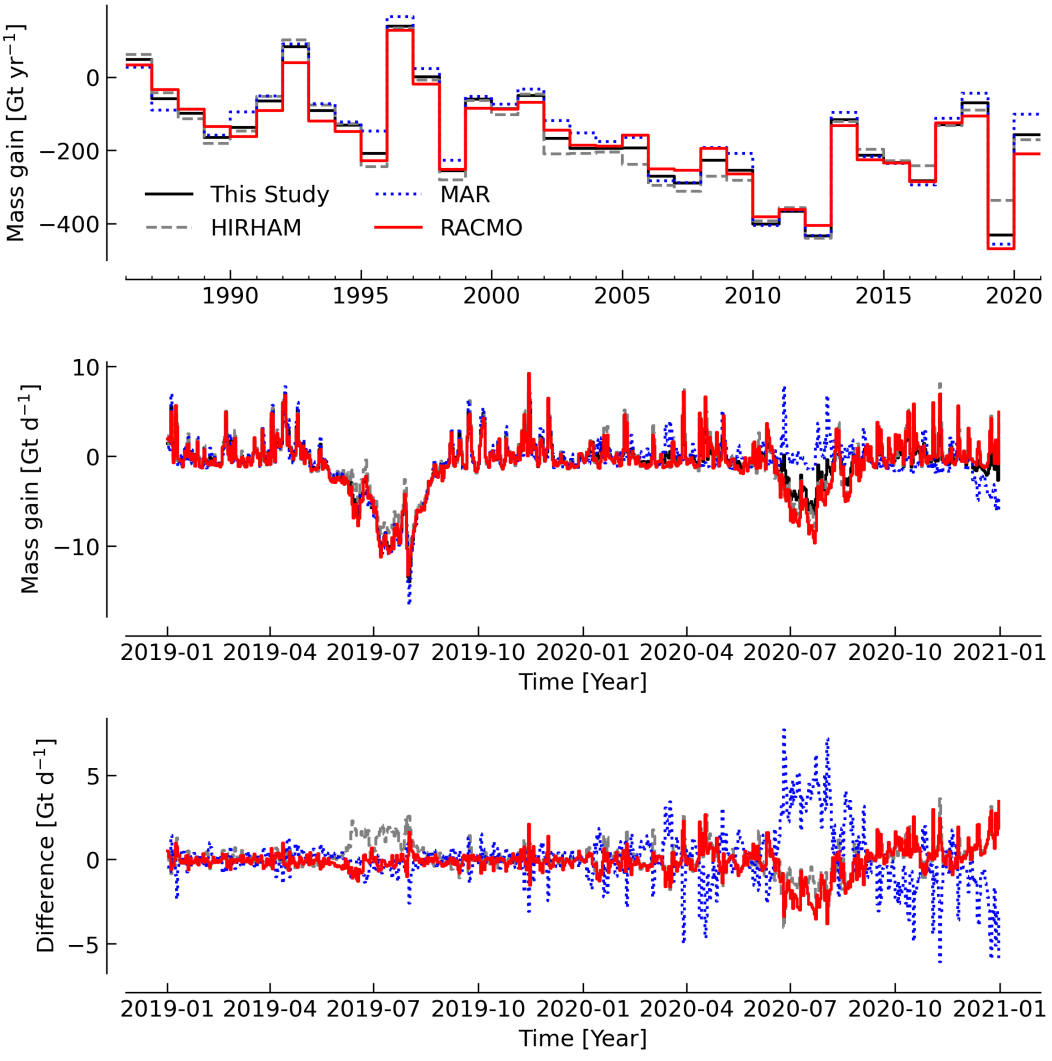

Figure A1. Comparison of This Study combined RCM product and the HIRHAM/HARMONIE, MAR, and RACMO RCMs. Results shown here are MB, not SMB, but the same MMB and BMB have been subtracted from each SMB product. Top panel: annual MB for entire time series. Middle panel: Example two years (2019 and 2020) at daily resolution. Bottom panel: Difference between the three RCM MB products and This Study RCM-averaged product, for the same data shown in the middle panel.

https://doi.org/10.5194/essd-2021-131
Preprint. Discussion started: 26 April 2021

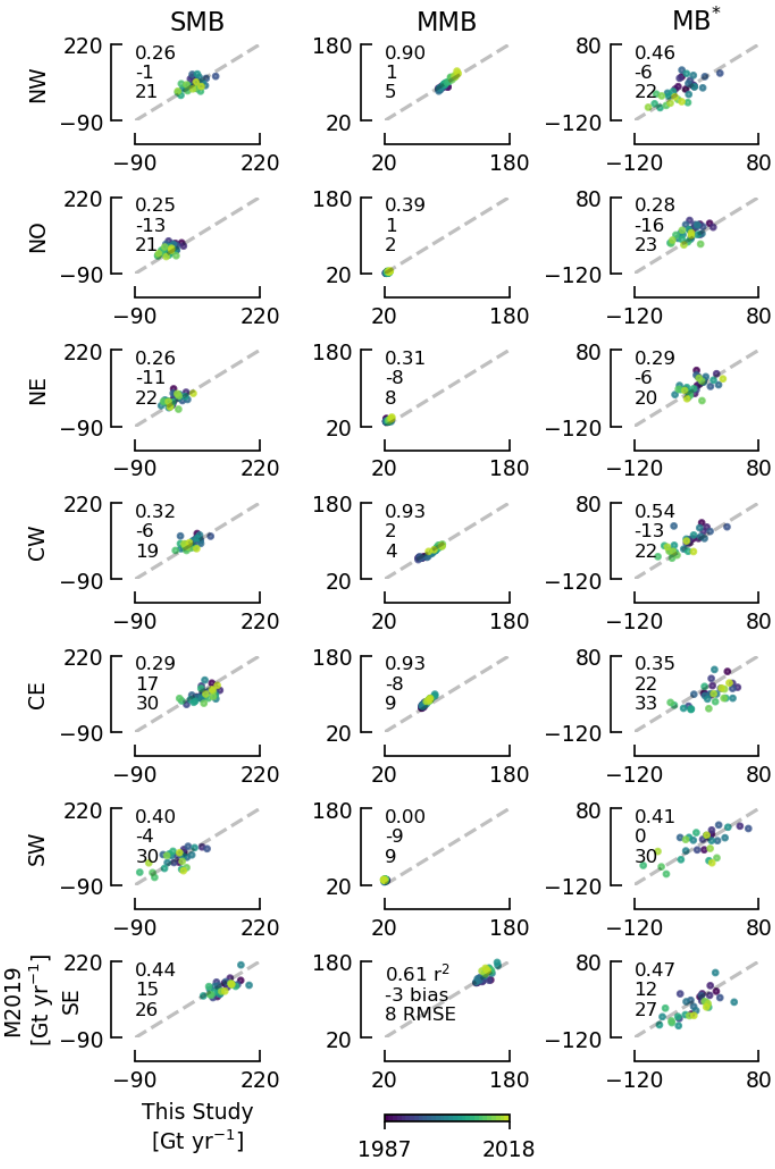

Appendix B: Mouginot 2019 by region

Figure B1. Comparison between This Study and Mouginot et al. (2019). Same data and display as Fig. 5 except here displayed by Mouginot and Rignot (2019) region. Numbers in each graph show r^2, bias, and RMSE, from top to bottom, respectively.

https://doi.org/10.5194/essd-2021-131
Preprint. Discussion started: 26 April 2021

Open Access Earth System Science Data Discussions

Appendix C: Colgan 2019 by sector

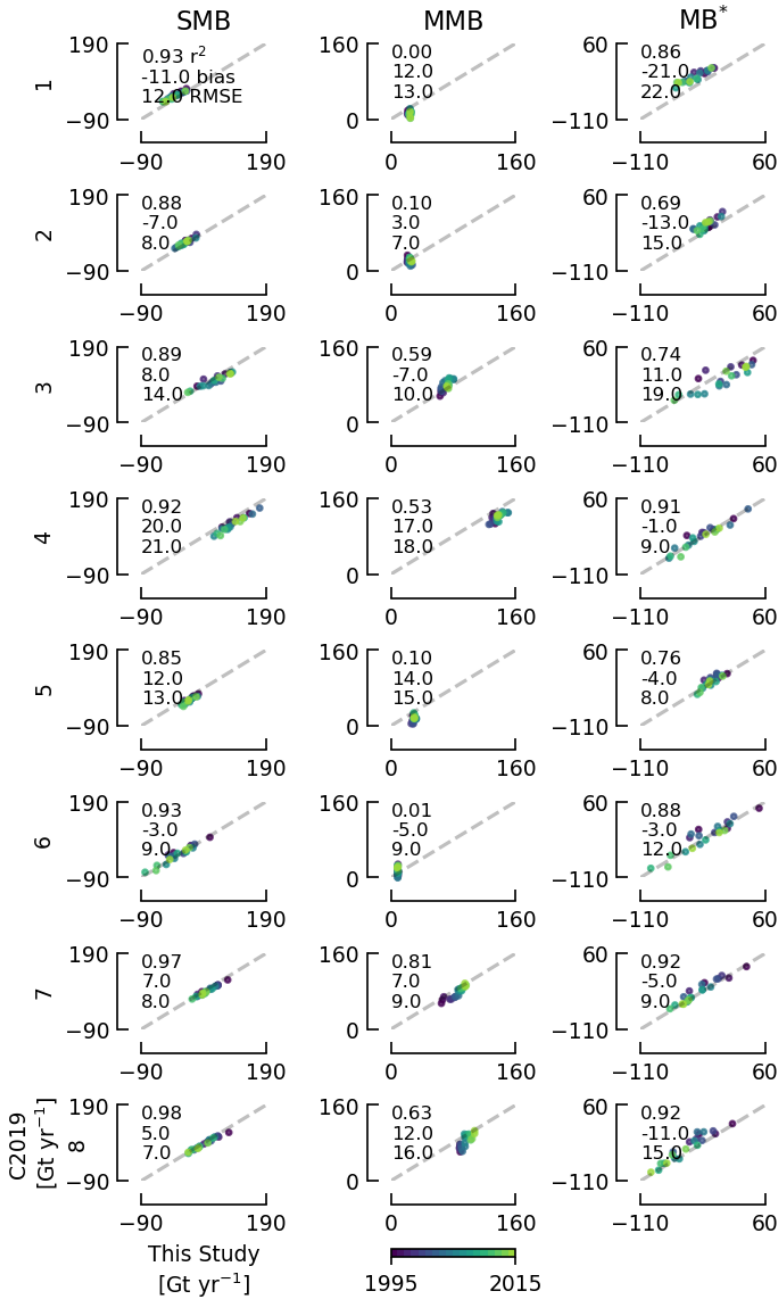

Figure C1. Comparison between This Study and Colgan et al. (2019). Same data and display as Fig. 6 except here displayed by Zwally et al. (2012) sector. Numbers in each graph show r^2, bias, and RMSE, from top to bottom, respectively.

https://doi.org/10.5194/essd-2021-131
Preprint. Discussion started: 26 April 2021

Open Access Earth System Science Data Discussions

Appendix D: Reconstructed runoff

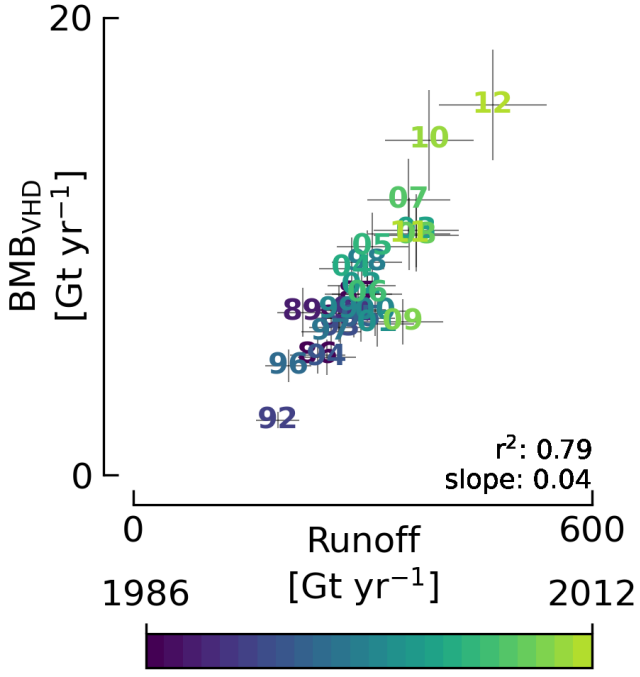

Figure D1. Comparison between MAR runoff and basal viscous heat dissipation derived from that runoff. The slope is used to estimate the reconstructed BMB_{VHD} from reconstructed runoff (see Sect. 5.3).

Appendix E: Software

This work was performed using only open-source software, primarily `GRASS GIS` (Neteler et al., 2012), CDO (Schulzweida, 2019), NCO (Zender, 2008), GDAL (GDAL/OGR contributors, 2020), and `Python` (Van Rossum and Drake Jr, 1995), in particular the `Jupyter` (Kluyver et al., 2016), `dask` (Dask Development Team, 2016; Rocklin, 2015), `pandas` (McKinney, 2010), `geopandas` (Jordahl et al., 2020), `numpy` (Oliphant, 2006), `x-array` (Hoyer and Hamman, 2017), and `Matplotlib` (Hunter, 2007) packages. The entire work was performed in `Emacs` (Stallman, 1981) using `Org Mode` (Schulte et al., 2012) on GNU/Linux and using many GNU utilities. The `parallel` (Tange, 2011) tool was used to speed up processing.

Author contributions. The following authors contributed in the following ways. Conceptualization: KDM, APA, and RSF. Curation: KDM, XF, PL, MS, KK, NBK, BN, MvdB, JB, and AS. Implementation: KDM, XF, PL, and KK. Funding: AS, APA, SBA, and RSF. SMB

https://doi.org/10.5194/essd-2021-131
Preprint. Discussion started: 26 April 2021

methods: XF, PL, BN, and MvdB. MMB methods: KDM, WC, AS, APA, and RSF. BMB methods: NBK and KDM. Validation (general): KDM. Validation GRACE: WC. Validation VC: WC and SS. Reconstruction methods: KK, JB, and KDM. Project admin: KDM, APA, SBA, and RSF. Resources: KDM, XF, PL, MS, KK, NBK, BN, MvdB, AS, and SBA. Software: KDM, XF, PL, and AS. Visualization: KDM. Writing: KDM, XF, PL, MS, KK, NBK, BN, MvdB, WC, SS, JB, APA, and RSF.

535 *Competing interests.* The authors declare that they have no conflict of interest.

Acknowledgements. Financial Support: Funding was provided by the Programme for Monitoring of the Greenland ice sheet (PROMICE). Parts of this work were funded by the INTAROS project under the European Union's Horizon 2020 research and innovation program under grant agreement no. 727890. B. Noël was funded by the NWO VENI grant VI.Veni.192.019.

https://doi.org/10.5194/essd-2021-131
Preprint. Discussion started: 26 April 2021

References

Barletta, V. R., Sørensen, L. S., and Forsberg, R.: Scatter of mass changes estimates at basin scale for Greenland and Antarctica, The Cryosphere, 7, 1411–1432, https://doi.org/10.5194/tc-7-1411-2013, 2013.

Barletta, V. R., Sørensen, L. S., Simonsen, S. B., and Forsberg, R.: Gravitational mass balance of Greenland 2003 to present v2.1, https://doi.org/10.11583/DTU.12866579.v1, 2020.

Bengtsson, L., Andrae, U., Aspelien, T., Batrak, Y., Calvo, J., de Rooy, W., Gleeson, E., Hansen-Sass, B., Homleid, M., Hortal, M., Ivarsson, K.-I., Lenderink, G., Niemelä, S., Nielsen, K. P., Onvlee, J., Rontu, L., Samuelsson, P., Muñoz, D. S., Subias, A., Tijm, S., Toll, V., Yang, X., and Køltzow, M. : The HARMONIE–AROME Model Configuration in the ALADIN–HIRLAM NWP System, Monthly Weather Review, 145, 1919–1935, https://doi.org/10.1175/mwr-d-16-0417.1, 2017.

Bolch, T., Sørensen, L. S., Simonsen, S. B., Mölg, N., Machguth, H., Rastner, P., and Paul, F.: Mass loss of Greenland's glaciers and ice caps 2003-2008 revealed from ICESat data, Geophysical Research Letters, 40, 875–881, https://doi.org/10.1002/grl.50270, 2013.

Bøssing Christensen, O., Drews, M., Hesselbjerg Christensen, J., Dethloff, K., Ketelsen, K., Hebestadt, I., and Rinke, A.: The HIRHAM Regional Climate Model. Version 5 (beta), no. 06-17 in Denmark. Danish Meteorological Institute. Technical Report, Danish Climate Centre, Danish Meteorological Institute, 2007.

Box, J., Colgan, W. T., and Kjeldsen, K.: Greenland SMB, D and TMB annual time series 1840-2012, https://doi.org/10.22008/FK2/L1QOZ5, https://doi.org/10.22008/FK2/L1QOZ5, 2021.

Box, J. E.: Greenland ice sheet mass balance reconstruction. Part II: surface mass balance (1840-2010), Journal of Climate, 26, 6974 – 6989, https://doi.org/10.1175/JCLI-D-12-00518.1, 2013.

Box, J. E. and Colgan, W.: Greenland ice sheet mass balance reconstruction. Part III: marine ice loss and total mass balance (1840-2010), Journal of Climate, 26, 6990 – 7002, https://doi.org/10.1175/JCLI-D-12-00546.1, 2013.

Box, J. E., Cressie, N., Bromwich, D. H., Jung, J.-H., van den Broeke, M. R., van Angelen, J. H., Forster, R. R., Miège, C., Mosley-Thompson, E., Vinther, B., and McConnell, J. R.: Greenland ice sheet mass balance reconstruction. Part I: Net snow accumulation (1600–2009), Journal of Climate, 26, 3919–3934, https://doi.org/10.1175/JCLI-D-12-00373.1, 2013.

Cappelen, J.: The observed climate of Greenland, 1958-99-with climatological standard normals, 1961-90, Danish Meteorological Institute, 2001.

Cappelen, J., Laursen, E. V., Jørgensen, P. V., and Kern-Hansen, C.: DMI Monthly Climate Data Collection 1768-2005: Denmark, The Faroe Islands and Greenland, DMI, 2006.

Cappelen, J., Laursen, E., Jørgensen, P., and Kern-Hansen, C.: DMI monthly climate data collection 1768-2010, Denmark, the Faroe Islands and Greenland, Tech. rep., DMI Technical Report 11-05. Copenhagen, 2011.

Citterio, M. and Ahlstrøm, A. P.: Brief communication "The aerophotogrammetric map of Greenland ice masses", The Cryosphere, 7, 445–449, https://doi.org/10.5194/tc-7-445-2013, 2013.

Colgan, W.: Greenland ice sheet mass balance assessment (1995-2019), https://doi.org/10.22008/FK2/XOTO3K, https://doi.org/10.22008/FK2/XOTO3K, 2021.

Colgan, W. and Arenson, L. U.: Open-Pit Glacier Ice Excavation: Brief Review, Journal of Cold Regions Engineering, 27, 223–243, https://doi.org/10.1061/(ASCE)CR.1943-5495.0000057, 2013.

Colgan, W., Mankoff, K. D., Kjeldsen, K. K., Bjørk, A. A., Box, J. E., Simonsen, S. B., Sørensen, L. S., Khan, S. A., Solgaard, A. M., Forsberg, R., Skourup, H., Stenseng, L., Kristensen, S. S., Hvidegaard, S. M., Citterio, M., Karlsson, N., Fettweis, X., Ahlstrøm, A. P.,

https://doi.org/10.5194/essd-2021-131
Preprint. Discussion started: 26 April 2021

Andersen, S. B., van As, D., and Fausto, R. S.: Greenland ice sheet mass balance assessed by PROMICE (1995 – 2015), Geological Survey of Denmark and Greenland Bulletin, 43, e2019430 201, https://doi.org/10.34194/GEUSB-201943-02-01, 2019.

Cuffey, K. M. and Paterson, W. S. B.: The physics of glaciers, Academic Press, fourth edn., 2010.

Dask Development Team: Dask: Library for dynamic task scheduling, https://dask.org, 2016.

Dee, D. P., Uppala, S. M., Simmons, A. J., Berrisford, P., Poli, P., Kobayashi, S., Andrae, U., Balmaseda, M. A., Balsamo, G., Bauer, P., Bechtold, P., Beljaars, A. C. M., van de Berg, I., Biblot, J., Bormann, N., Delsol, C., Dragani, R., Fuentes, M., Greer, A. J., Haimberger, L., Healy, S. B., Hersbach, H., Holm, E. V., Isaksen, L., Kallberg, P., Kohler, M., Matricardi, M., McNally, A. P., Mong-Sanz, B. M., Morcette, J.-J., Park, B.-K., Peubey, C., de Rosnay, P., Tavolato, C., Thepaut, J. N., , and Vitart, F.: The ERA-Interim reanalysis: configuration and performance of the data assimilation system, Quarterly Journal of the Royal Meteorological Society, 137, 553–597, https://doi.org/10.1002/qj.828, 2011.

Eerola, K.: About the performance of HIRLAM version 7.0, Hirlam Newsletter, 51, 93–102, 2006.

Enderlin, E. M., Howat, I. M., Jeong, S., Noh, M.-J., van Angelen, J. H., and van den Broeke, M. R.: An improved mass budget for the Greenland Ice Sheet, Geophysical Research Letters, 41, 866–872, https://doi.org/10.1002/2013GL059010, 2014.

Ettema, J., van den Broeke, M. R., van Meijgaard, E., van de Berg, W. J., Box, J. E., and Steffen, K.: Climate of the Greenland ice sheet using a high-resolution climate model – Part 1: Evaluation, The Cryosphere, 4, 511–527, https://doi.org/10.5194/tc-4-511-2010, 2010.

Fettweis, X., Box, J. E., Agosta, C., Amory, C., Kittel, C., Lang, C., Van As, D., Machguth, H., and Gallée, H.: Reconstructions of the 1900–2015 Greenland ice sheet surface mass balance using the regional climate MAR model, The Cryosphere, 11, 1015–1033, https://doi.org/10.5194/tc-11-1015-2017, 2017.

Fettweis, X., Hofer, S., Krebs-Kanzow, U., Amory, C., Aoki, T., Berends, C. J., Born, A., Box, J. E., Delhasse, A., Fujita, K., Gierz, P., Goelzer, H., Hanna, E., Hashimoto, A., Huybrechts, P., Kapsch, M.-L., King, M. D., Kittel, C., Lang, C., Langen, P. L., Lenaerts, J. T. M., Liston, G. E., Lohmann, G., Mernild, S. H., Mikolajewicz, U., Modali, K., Mottram, R. H., Niwano, M., Noël, B., Ryan, J. C., Smith, A., Streffing, J., Tedesco, M., van de Berg, W. J., van den Broeke, M., van de Wal, R. S. W., van Kampenhout, L., Wilton, D., Wouters, B., Ziemen, F., and Zolles, T.: GrSMBMIP: intercomparison of the modelled 1980–2012 surface mass balance over the Greenland Ice Sheet, The Cryosphere, 14, 3935–3958, https://doi.org/10.5194/tc-14-3935-2020, 2020.

Fox Maule, C., Purucker, M. E., and Olsen, N.: Inferring magnetic crustal thickness and geothermal heat flux from crustal magnetic field models, 2009.

Gardner, A. S., Moholdt, G., Cogley, J. G., Wouters, B., Arendt, A. A., Wahr, J., Berthier, E., Hock, R., Pfeffer, W. T., Kaser, G., Ligtenberg, S. R. M., Bolch, T., Sharp, M. J., Hagen, J. O., Van Den Broeke, M. R., and Paul, F.: A Reconciled Estimate of Glacier Contributions to Sea Level Rise: 2003 to 2009, Science, 340, 852–857, https://doi.org/10.1126/science.1234532, 2013.

GDAL/OGR contributors: GDAL/OGR Geospatial Data Abstraction software Library, Open Source Geospatial Foundation, https://gdal.org, 2020.

Gillet-Chaulet, F., Gagliardini, O., Seddik, H., Nodet, M., Durand, G., Ritz, C., Zwinger, T., Greve, R., and Vaughan, D. G.: Greenland ice sheet contribution to sea-level rise from a new-generation ice-sheet model, The Cryosphere, 6, 1561–1576, https://doi.org/10.5194/tc-6-1561-2012, 2012.

Groh, A., Horwath, M., Horvath, A., Meister, R., Sørensen, L. S., Barletta, V. R., Forsberg, R., Wouters, B., Ditmar, P., Ran, J., Klees, R., Su, X., Shang, K., Guo, J., Shum, C. K., Schrama, E., and Shepherd, A.: Evaluating GRACE Mass Change Time Series for the Antarctic and Greenland Ice Sheet – Methods and Results, Geosciences, 9, 415, https://doi.org/10.3390/geosciences9100415, https://doi.org/10.3390/geosciences9100415, 2019.

https://doi.org/10.5194/essd-2021-131
Preprint. Discussion started: 26 April 2021

Hersbach, H., Bell, B., Berrisford, P., Hirahara, S., Horányi, A., Muñoz-Sabater, J., Nicolas, J., Peubey, C., Radu, R., Schepers, D., Simmons, A., Soci, C., Abdalla, S., Abellan, X., Balsamo, G., Bechtold, P., Biavati, G., Bidlot, J., Bonavita, M., Chiara, G. D., Dahlgren, P., Dee, D., Diamantakis, M., Dragani, R., Flemming, J., Forbes, R., Fuentes, M., Geer, A., Haimberger, L., Healy, S., Hogan, R. J., Hólm, E., Janisková, M., Keeley, S., Laloyaux, P., Lopez, P., Lupu, C., Radnoti, G., de Rosnay, P., Rozum, I., Vamborg, F., Villaume, S., and Thépaut, J.: The ERA5 global reanalysis, Quarterly Journal of the Royal Meteorological Society, 146, 1999–2049, https://doi.org/10.1002/qj.3803, 2020.

Howat, I. M., Negrete, A., and Smith, B. E.: The Greenland Ice Mapping Project (GIMP) land classification and surface elevation data sets, The Cryosphere, 8, 1509–1518, https://doi.org/10.5194/tc-8-1509-2014, 2014.

Hoyer, S. and Hamman, J. J.: xarray: N-D labeled Arrays and Datasets in Python, Journal of Open Research Software, 5, https://doi.org/10.5334/jors.148, http://dx.doi.org/10.5334/jors.148, 2017.

Hunter, J. D.: Matplotlib: A 2D graphics environment, Computing In Science Engineering, 9, 90–95, 2007.

Jordahl, K., den Bossche, J. V., Wasserman, J., McBride, J., Fleischmann, M., Gerard, J., Tratner, J., Perry, M., Farmer, C., Hjelle, G. A., Gillies, S., Cochran, M., Bartos, M., Culbertson, L., Eubank, N., Bilogur, A., and maxalbert: geopandas/geopandas: v0.7.0, https://doi.org/10.5281/zenodo.3669853, https://doi.org/10.5281/zenodo.3669853, 2020.

Joughin, I., Smith, B. E., and Howat, I.: Greenland Ice Mapping Project: ice flow velocity variation at sub-monthly to decadal timescales, The Cryosphere, 12, 2211–2227, https://doi.org/10.5194/tc-12-2211-2018, 2018.

Karlsson, N. B.: Greenland Ice Sheet Basal Melt, https://doi.org/10.22008/FK2/PLNUEO, https://doi.org/10.22008/FK2/PLNUEO, 2021.

Karlsson, N. B., Solgaard, A. M., Mankoff, K. D., Box, J. E., Citterio, M., Colgan, W. T., Larsen, S. H., Kjeldsen, K. K., Korsgaard, N. J., Benn, D. I., Hewitt, I., and Fausto, R. S.: A First Constraint on Basal Melt-water Production of the Greenland Ice Sheet, Nature Communications, **Accepted**, 2021.

Khan, S. A., Sasgen, I., Bevis, M., van Dam, T., Bamber, J. L., Wahr, J., Willis, M., Kjær, K. H., Wouters, B., Helm, V., Csatho, B., Fleming, K., Bjørk, A. A., Aschwanden, A., Knudsen, P., and Munneke, P. K.: Geodetic measurements reveal similarities between post-Last Glacial Maximum and present-day mass loss from the Greenland ice sheet, Science Advances, 2, e1600 931–e1600 931, https://doi.org/10.1126/sciadv.1600931, 2016.

King, M. D., Howat, I. M., Jeong, S., Noh, M. J., Wouters, B., Noël, B., and van den Broeke, M. R.: Seasonal to decadal variability in ice discharge from the Greenland Ice Sheet, The Cryosphere, 12, 3813–3825, https://doi.org/10.5194/tc-12-3813-2018, 2018.

Kjeldsen, K. K., Korsgaard, N. J., Bjørk, A. A., Khan, S. A., Box, J. E., Funder, S., Larsen, N. K., Bamber, J. L., Colgan, W., Broeke, M. v. d., Siggaard-Andersen, M.-L., Nuth, C., Schomacker, A., Andresen, C. S., Willerslev, E., and Kjær, K. H.: Spatial and temporal distribution of mass loss from the Greenland Ice Sheet since AD 1900, Nature, 528, 396–400, https://doi.org/10.1038/nature16183, 2015.

Kjeldsen, K. K., Khan, S. A., Colgan, W. T., MacGregor, J. A., and Fausto, R. S.: Time-Varying Ice Sheet Mask: Implications on Ice-Sheet Mass Balance and Crustal Uplift, Journal of Geophysical Research: Earth Surface, 125, https://doi.org/10.1029/2020jf005775, 2020.

Kluyver, T., Ragan-Kelley, B., Pérez, F., Granger, B., Bussonnier, M., Frederic, J., Kelley, K., Hamrick, J., Grout, J., Corlay, S., Ivanov, P., Avila, D., Abdalla, S., and Willing, C.: Jupyter Notebooks – a publishing format for reproducible computational workflows, https://doi.org/10.3233/978-1-61499-649-1-87, 2016.

Langen, P. L., Fausto, R. S., Vandecrux, B., Mottram, R. H., and Box, J. E.: Liquid Water Flow and Retention on the Greenland Ice Sheet in the Regional Climate Model HIRHAM5: Local and Large-Scale Impacts, Frontiers in Earth Science, 4, https://doi.org/10.3389/feart.2016.00110, 2017.

https://doi.org/10.5194/essd-2021-131
Preprint. Discussion started: 26 April 2021

Laprise, R.: The Euler Equations of Motion with Hydrostatic Pressure as an Independent Variable, Monthly Weather Review, 120, 197–207, https://doi.org/10.1175/1520-0493(1992)120<0197:teeomw>2.0.co;2, 1992.

Lefebre, F.: Modeling of snow and ice melt at ETH Camp (West Greenland): A study of surface albedo, Journal of Geophysical Research, 108, https://doi.org/10.1029/2001jd001160, 2003.

Lenaerts, J. T. M., van den Broeke, M. R., van Angelen, J. H., van Meijgaard, E., and Déry, S. J.: Drifting snow climate of the Greenland ice sheet: a study with a regional climate model, The Cryosphere, 6, 891–899, https://doi.org/10.5194/tc-6-891-2012, 2012.

Lewis, G., Osterberg, E., Hawley, R., Whitmore, B., Marshall, H. P., and Box, J.: Regional Greenland accumulation variability from Operation IceBridge airborne accumulation radar, The Cryosphere, 11, 773–788, https://doi.org/10.5194/tc-11-773-2017, 2017.

Lewis, G., Osterberg, E., Hawley, R., Marshall, H. P., Meehan, T., Graeter, K., McCarthy, F., Overly, T., Thundercloud, Z., and Ferris, D.: Recent precipitation decrease across the western Greenland ice sheet percolation zone, The Cryosphere, 13, 2797–2815, https://doi.org/10.5194/tc-13-2797-2019, 2019.

Liestøl, O.: Glacier Dammed Lakes in Norway, vol. 81, Fabritius Sønners Forlag, Oslo, 1956.

Ligtenberg, S. R. M., Kuipers Munneke, P., Noël, B. P. Y., and van den Broeke, M. R.: Brief communication: Improved simulation of the present-day Greenland firn layer (1960–2016), The Cryosphere, 12, 1643–1649, https://doi.org/10.5194/tc-12-1643-2018, 2018.

Lucas-Picher, P., Wulff-Nielsen, M., Christensen, J. H., Aðalgeirsdóttir, G., Mottram, R., and Simonsen, S. B.: Very high resolution regional climate model simulations over Greenland: Identifying added value, Journal of Geophysical Research: Atmospheres, 117, https://doi.org/10.1029/2011jd016267, 2012.

MacGregor, J. A., Fahnestock, M. A., Catania, G. A., Aschwanden, A., Clow, G. D., Colgan, W. T., Gogineni, P. S., Morlighem, M., Nowicki, S. M. J., Paden, J. D., Price, S. F., and Seroussi, H.: A synthesis of the basal thermal state of the Greenland Ice Sheet, Journal of Geophysical Research: Earth Surface, 121, 1328–1350, https://doi.org/10.1002/2015JF003803, 2016.

Maier, N., Humphrey, N., Harper, J., and Meierbachtol, T.: Sliding dominates slow-flowing margin regions, Greenland Ice Sheet, Science Advances, 5, eaaw5406, https://doi.org/10.1126/sciadv.aaw5406, 2019.

Maier, N., Gimbert, F., Gillet-Chaulet, F., and Gilbert, A.: Basal traction mainly dictated by hard-bed physics over grounded regions of Greenland, The Cryosphere, 15, 1435–1451, https://doi.org/10.5194/tc-15-1435-2021, 2021.

Mankoff, K.: Greenland Ice Sheet solid ice discharge from 1986 through last month: Gates, https://doi.org/10.22008/promice/data/ice_discharge/gates/v02, https://doi.org/10.22008/promice/data/ice_discharge/gates/v02, 2020.

Mankoff, K. and Solgaard, A.: Greenland Ice Sheet solid ice discharge from 1986 through last month: Discharge, https://doi.org/10.22008/promice/data/ice_discharge/d/v02, https://doi.org/10.22008/promice/data/ice_discharge/d/v02, 2020a.

Mankoff, K. and Solgaard, A.: Ice Discharge, https://dataverse01.geus.dk/dataverse/ice_discharge, 2020b.

Mankoff, K., Fettweis, X., Solgaard, A., Langen, P., Stendel, M., Noël, B., van den Broeke, M. R., Karlsson, N., Box, J. E., and Kjeldsen, K.: Greenland ice sheet mass balance from from 1840 through next week, https://doi.org/10.22008/FK2/YG3IWC, 2021.

Mankoff, K. D. and Tulaczyk, S. M.: The past, present, and future viscous heat dissipation available for Greenland subglacial conduit formation, The Cryosphere, 11, 303–317, https://doi.org/10.5194/tc-11-303-2017, 2017.

Mankoff, K. D., Noël, B., Fettweis, X., Ahlstrøm, A. P., Colgan, W., Kondo, K., Langley, K., Sugiyama, S., van As, D., and Fausto, R. S.: Greenland liquid water discharge from 1958 through 2019, Earth System Science Data, 12, 2811–2841, https://doi.org/10.5194/essd-12-2811-2020, 2020a.

https://doi.org/10.5194/essd-2021-131
Preprint. Discussion started: 26 April 2021

Mankoff, K. D., Solgaard, A., Colgan, W., Ahlstrøm, A. P., Khan, S. A., and Fausto, R. S.: Greenland Ice Sheet solid ice discharge from 1986 through March 2020, Earth System Science Data, 12, 1367–1383, https://doi.org/10.5194/essd-12-1367-2020, 2020b.

Martos, Y. M., Jordan, T. A., Catalán, M., Jordan, T. M., Bamber, J. L., and Vaughan, D. G.: Geothermal Heat Flux Reveals the Iceland Hotspot Track Underneath Greenland, Geophysical Research Letters, https://doi.org/10.1029/2018gl078289, 2018.

McKinney, W.: Data Structures for Statistical Computing in Python, in: Proceedings of the 9th Python in Science Conference, edited by van der Walt, S. and Millman, J., pp. 51 – 56, https://doi.org/10.25080/Majora-92bf1922-00a, 2010.

Millan, R., Rignot, E., Mouginot, J., Wood, M., Bjørk, A. A., and Morlighem, M.: Vulnerability of Southeast Greenland glaciers to warm Atlantic Water from Operation IceBridge and Ocean Melting Greenland data., Geophysical Research Letters, 45, 2688–2696, https://doi.org/10.1002/2017gl076561, 2018.

Morlighem, M., Williams, C., Rignot, E., An, L., Arndt, J. E., Bamber, J., Catania, G., Chauché, N., Dowdeswell, J. A., Dorschel, B., Fenty, I., Hogan, K., Howat, I., Hubbard, A., Jakobsson, M., Jordan, T. M., Kjeldsen, K. K., Millan, R., Mayer, L., Mouginot, J., Noël, B., O'Cofaigh, C., Palmer, S. J., Rysgaard, S., Seroussi, H., Siegert, M. J., Slabon, P., Straneo, F., van den Broeke, M. R., Weinrebe, W., Wood, M., and Zinglersen, K.: IceBridge BedMachine Greenland, Version 3, https://doi.org/10.5067/2CIX82HUV88Y, used all subsets; Accessed 2018-10-28, 2017a.

Morlighem, M., Williams, C. N., Rignot, E., An, L., Arndt, J. E., Bamber, J. L., Catania, G., Chauché, N., Dowdeswell, J. A., Dorschel, B., Fenty, I., Hogan, K., Howat, I. M., Hubbard, A., Jakobsson, M., Jordan, T. M., Kjeldsen, K. K., Millan, R., Mayer, L., Mouginot, J., Noël, B. P. Y., Cofaigh, C. Ó., Palmer, S., Rysgaard, S., Seroussi, H., Siegert, M. J., Slabon, P., Straneo, F., van den Broeke, M. R., Weinrebe, W., Wood, M., and Zinglersen, K. B.: BedMachine v3: Complete bed topography and ocean bathymetry mapping of Greenland from multi-beam echo sounding combined with mass conservation, Geophysical Research Letters, 44, https://doi.org/10.1002/2017gl074954, 2017b.

Mouginot, J. and Rignot, E.: Glacier catchments/basins for the Greenland Ice Sheet, https://doi.org/10.7280/d1wt11, https://dash.lib.uci.edu/stash/dataset/doi:10.7280/D1WT11, 2019.

Mouginot, J., Rignot, E., Bjørk, A. A., van den Broeke, M., Millan, R., Morlighem, M., Noël, B., Scheuchl, B., and Wood, M.: Forty-six years of Greenland Ice Sheet mass balance from 1972 to 2018, Proceedings of the National Academy of Sciences, p. 201904242, https://doi.org/10.1073/pnas.1904242116, 2019.

Neteler, M., Bowman, M. H., Landa, M., and Metz, M.: GRASS GIS: a multi-purpose Open Source GIS, Environmental Modelling Software, 31, 124–130, https://doi.org/10.1016/j.envsoft.2011.11.014, 2012.

Nilsson, J., Vallelonga, P., Simonsen, S. B., Sørensen, L. S., Forsberg, R., Dahl-Jensen, D., Hirabayashi, M., Goto-Azuma, K., Hvidberg, C. S., Kjær, H. A., et al.: Greenland 2012 melt event effects on CryoSat-2 radar altimetry, Geophysical Research Letters, 42, 3919–3926, 2015.

Noël, B., van de Berg, W. J., Machguth, H., Lhermitte, S., Howat, I., Fettweis, X., and van den Broeke, M. R.: A daily, 1 km resolution data set of downscaled Greenland ice sheet surface mass balance (1958–2015), The Cryosphere, 10, 2361–2377, https://doi.org/10.5194/tc-10-2361-2016, 2016.

Noël, B., van de Berg, W. J., van Wessem, J. M., van Meijgaard, E., van As, D., Lenaerts, J. T. M., Lhermitte, S., Kuipers Munneke, P., Smeets, C. J. P. P., van Ulft, L. H., van de Wal, R. S. W., and ven den Broeke, M. R.: Modelling the climate and surface mass balance of polar ice sheets using RACMO2 – Part 1: Greenland (1958–2016), The Cryosphere, 12, 811–831, https://doi.org/10.5194/tc-12-811-2018, 2018.

https://doi.org/10.5194/essd-2021-131
Preprint. Discussion started: 26 April 2021

Noël, B., van de Berg, W. J., Lhermitte, S., and van den Broeke, M. R.: Rapid ablation zone expansion amplifies north Greenland mass loss, Science Advances, 5, eaaw0123, https://doi.org/10.1126/sciadv.aaw0123, 2019.

Oliphant, T. E.: A guide to NumPy, vol. 1, Trelgol Publishing USA, 2006.

Pfeffer, W. T., Meier, M. F., and Illangasekare, T. H.: Retention of Greenland runoff by refreezing: Implications for projected future sea level change, Journal of Geophysical Research, 96, 22 117, https://doi.org/10.1029/91jc02502, 1991.

Rastner, P., Bolch, T., Mölg, N., Machguth, H., Le Bris, R., and Paul, F.: The first complete inventory of the local glaciers and ice caps on Greenland, The Cryosphere, 6, 1483–1495, https://doi.org/10.5194/tc-6-1483-2012, 2012.

Rezvanbehbahani, S., Stearns, L. A., van der Veen, C. J., Oswald, G. K. A., and Greve, R.: Constraining the geothermal heat flux in Greenland at regions of radar-detected basal water, Journal of Glaciology, 65, 1023–1034, https://doi.org/10.1017/jog.2019.79, 2019.

Rignot, E., Mouginot, J., Scheuchl, B., van den Broeke, M., van Wessem, M. J., and Morlighem, M.: Four decades of Antarctic Ice Sheet mass balance from 1979–2017, Proceedings of the National Academy of Sciences, 116, 1095–1103, https://doi.org/10.1073/pnas.1812883116, http://dx.doi.org/10.1073/pnas.1812883116, 2019.

Rocklin, M.: Dask: Parallel Computation with Blocked algorithms and Task Scheduling, in: Proceedings of the 14th Python in Science Conference, edited by Huff, K. and Bergstra, J., pp. 130 – 136, 2015.

Roeckner, E., Bäuml, G., Bonaventura, L., Brokopf, R., Esch, M., Giorgetta, M., Hagemann, S., Kirchner, I., Kornblueh, L., Manzini, E., et al.: The atmospheric general circulation model ECHAM 5. Part I: Model description, 2003.

Rogozhina, I., Hagedoorn, J. M., Martinec, Z., Fleming, K., Soucek, O., Greve, R., and Thomas, M.: Effects of uncertainties in the geothermal heat flux distribution on the Greenland Ice Sheet: An assessment of existing heat flow models, Journal of Geophysical Research: Earth Surface, 117, https://doi.org/10.1029/2011JF002098, 2012.

Ryser, C., Lüthi, M. P., Andrews, L. C., Hoffman, M. J., Catania, G. A., Hawley, R. L., Neumann, T. A., and Kristensen, S. S.: Sustained high basal motion of the Greenland ice sheet revealed by borehole deformation, Journal of Glaciology, 60, 647 – 660, https://doi.org/10.3189/2014JoG13J196, 2014.

Sasgen, I., Van Den Broeke, M., Bamber, J. L., Rignot, E., Sørensen, L. S., Wouters, B., Martinec, Z., Velicogna, I., and Simonsen, S. B.: Timing and origin of recent regional ice-mass loss in Greenland, Earth and Planetary Science Letters, 333-334, 293–303, https://doi.org/10.1016/j.epsl.2012.03.033, 2012.

Schulte, E., Davison, D., Dye, T., and Dominik, C.: A multi-language computing environment for literate programming and reproducible research, Journal of Statistical Software, 46, 1–24, 2012.

Schulzweida, U.: CDO User Guide, https://doi.org/10.5281/zenodo.3539275, https://doi.org/10.5281/zenodo.3539275, 2019.

Shapiro, N. M. and Ritzwoller, M. H.: Inferring Surface Heat Flux Distributions Guided by a Global Seismic Model: Particular Application to Antarctica, Earth and Planetary Science Letters, 223, 213–224, https://doi.org/10.1016/j.epsl.2004.04.011, 2004.

Shreve, R. L.: Movement of water in glaciers, Journal of Glaciology, 11, 205–214, 1972.

Simmons, A. J. and Burridge, D. M.: An Energy and Angular-Momentum Conserving Vertical Finite-Difference Scheme and Hybrid Vertical Coordinates, Monthly Weather Review, 109, 758–766, https://doi.org/10.1175/1520-0493(1981)109<0758:aeaamc>2.0.co;2, 1981.

Simonsen, S. B., Barletta, V. R., Colgan, W., and Sørensen, L. S.: Greenland Ice Sheet mass balance (1992-2020) from calibrated radar altimetry, Geophysical Research Letters, https://doi.org/10.1029/2020gl091216, see http://doi.org/10.11583/DTU.13353062. See citet:simonsen$_2$021$_d$$ata, 2021a$.

https://doi.org/10.5194/essd-2021-131
Preprint. Discussion started: 26 April 2021

Simonsen, S. B., Barletta, V. R., Colgan, W., and Sørensen, L. S.: Greenland Ice Sheet mass balance (1992-2020) from calibrated radar altimetry, https://doi.org/10.11583/DTU.13353062.v1, https://data.dtu.dk/articles/dataset/Greenland_Ice_Sheet_mass_balance_1992-2020_from_calibrated_radar_altimetry/13353062, see http://doi.org/10.1029/2020GL091216. See citet:simonsen$_2$021, 2021b.

Smith, B., Fricker, H. A., Gardner, A. S., Medley, B., Nilsson, J., Paolo, F. S., Holschuh, N., Adusumilli, S., Brunt, K., Csatho, B., and et al.: Pervasive ice sheet mass loss reflects competing ocean and atmosphere processes, Science, p. eaaz5845, https://doi.org/10.1126/science.aaz5845, 2020.

Solgaard, A. and Kusk, A.: Greenland Ice Velocity from Sentinel-1 Edition 2, https://doi.org/10.22008/promice/data/sentinel1icevelocity/greenlandicesheet, 2021.

Solgaard, A., Kusk, A., Boncori, J. P. M., Dall, J., Mankoff, K. D., Ahlstrøm, A. P., Andersen, S. B., Citterio, M., Karlsson, N. B., Kjeldsen, K. K., and et al.: Greenland ice velocity maps from the PROMICE project, Earth System Science Discussions, https://doi.org/10.5194/essd-2021-46, 2021.

Stallman, R. M.: EMACS the Extensible, Customizable Self-Documenting Display Editor, in: Proceedings of the ACM SIGPLAN SIGOA Symposium on Text Manipulation, p. 147–156, Association for Computing Machinery, New York, NY, USA, https://doi.org/10.1145/800209.806466, https://doi.org/10.1145/800209.806466, 1981.

Sutterley, T. C., Velicogna, I., Rignot, E. J., Mouginot, J., Flament, T., van den Broeke, M. R., van Wessem, J. M., and Reijmer, C. H.: Mass loss of the Amundsen Sea Embayment of West Antarctica from four independent techniques, Geophysical Research Letters, 41, 8421–8428, https://doi.org/10.1002/2014GL061940, 2014.

Sørensen, L. S., Simonsen, S. B., Nielsen, K., Lucas-Picher, P., Spada, G., Adalgeirsdottir, G., Forsberg, R., and Hvidberg, C. S.: Mass balance of the Greenland ice sheet (2003–2008) from ICESat data – the impact of interpolation, sampling and firn density, The Cryosphere, 5, 173–186, https://doi.org/10.5194/tc-5-173-2011, http://dx.doi.org/10.5194/tc-5-173-2011, 2011.

Tange, O.: GNU Parallel - The Command-Line Power Tool, ;login: The USENIX Magazine, 36, 42–47, https://doi.org/10.5281/zenodo.16303, http://www.gnu.org/s/parallel, 2011.

Tedesco, M. and Fettweis, X.: Unprecedented atmospheric conditions (1948–2019) drive the 2019 exceptional melting season over the Greenland ice sheet, The Cryosphere, 14, 1209–1223, https://doi.org/10.5194/tc-14-1209-2020, 2020.

The IMBIE Team: Mass balance of the Greenland Ice Sheet from 1992 to 2018, Nature, 579, 233–239, https://doi.org/10.1038/s41586-019-1855-2, http://dx.doi.org/10.1038/s41586-019-1855-2, 2019.

Uppala, S. M., Kållberg, P. W., Simmons, A. J., Andrae, U., Da Costa Bechtold, V., Fiorino, M., Gibson, J., Haseler, J., Hernandez, A., Kelly, G. A., Li, X., Onogi, K., Saarinen, S., Sokka, N., Allan, R. P., Anderson, E., Arpe, K., Balmaseda, M. A., Beljaars, A. C. M., Van De Berg, L., Bidlot, J., Bormann, N., Caires, S., Chevallier, F., Dethof, A., Dragosavac, M., Fisher, M., Fuentes, M., Hagemann, S., Hólm, E., Hoskins, B. J., Isaksen, L., Janssen, P. A. E. M., Jenne, R., Mcnally, A. P., Mahfouf, J.-F., Morcrette, J.-J., Rayner, N. A., Saunders, R. W., Simon, P., Sterl, A., Trenbreth, K. E., Untch, A., Vasiljevic, D., Viterbo, P., , and Woollen, J.: The ERA-40 re-analysis, Quarterly Journal of the Royal Meteorological Society, 131, 2961–3012, https://doi.org/10.1256/qj.04.176, 2005.

van Angelen, J. H., Lenaerts, J. T. M., Lhermitte, S., Fettweis, X., Kuipers Munneke, P., van den Broeke, M. R., van Meijgaard, E., and Smeets, C. J. P. P.: Sensitivity of Greenland Ice Sheet surface mass balance to surface albedo parameterization: a study with a regional climate model, The Cryosphere, 6, 1175–1186, https://doi.org/10.5194/tc-6-1175-2012, 2012.

van de Berg, W. J. and Medley, B.: Brief Communication: Upper-air relaxation in RACMO2 significantly improves modelled interannual surface mass balance variability in Antarctica, The Cryosphere, 10, 459–463, https://doi.org/10.5194/tc-10-459-2016, 2016.

Van Rossum, G. and Drake Jr, F. L.: Python reference manual, Centrum voor Wiskunde en Informatica Amsterdam, 1995.

https://doi.org/10.5194/essd-2021-131
Preprint. Discussion started: 26 April 2021

Velicogna, I., Mohajerani, Y., A, G., Landerer, F., Mouginot, J., Noel, B., Rignot, E., Sutterley, T., Broeke, M., Wessem, M., and et al.: Continuity of Ice Sheet Mass Loss in Greenland and Antarctica From the GRACE and GRACE Follow-On Missions, Geophysical Research Letters, 47, https://doi.org/10.1029/2020gl087291, 2020.

Vinther, B. M., Andersen, K. K., Jones, P. D., Briffa, K. R., and Cappelen, J.: Extending Greenland temperature records into the late eighteenth century, Journal of Geophysical Research, 111, https://doi.org/10.1029/2005jd006810, http://dx.doi.org/10.1029/2005JD006810, 2006.

Zemp, M., Huss, M., Eckert, N., Thibert, E., Paul, F., Nussbaumer, S. U., and Gärtner-Roer, I.: Brief communication: Ad hoc estimation of glacier contributions to sea-level rise from the latest glaciological observations, The Cryosphere, 14, 1043–1050, https://doi.org/10.5194/tc-14-1043-2020, 2020.

Zender, C. S.: Analysis of self-describing gridded geoscience data with netCDF Operators (NCO), Environmental Modelling & Software, 23, 1338–1342, https://doi.org/10.1016/j.envsoft.2008.03.004, https://doi.org/10.1016/j.envsoft.2008.03.004, 2008.

Zuo, Z. and Oerlemans, J.: Modelling albedo and specific balance of the Greenland ice sheet: calculations for the Søndre Strømfjord transect, Journal of Glaciology, 42, 305–317, https://doi.org/10.3189/s0022143000004160, 1996.

Zwally, H. J. and Giovinetto, M. B.: Overview and Assessment of Antarctic Ice-Sheet Mass Balance Estimates: 1992–2009, Surveys in Geophysics, 32, 1–26, https://doi.org/10.1007/s10712-011-9123-5, 2011.

Zwally, H. J., Giovinetto, M. B., Beckley, M. A., and Saba, J. L.: Antarctic and Greenland Drainage Systems, http://icesat4.gsfc.nasa.gov/cryo_data/ant_grn_drainage_systems.php, GSFC Cryospheric Sciences Laboratory, 2012.